LIGO Laboratory / LIGO Scientific Collaboration

LIGO- **T1100258**-v4 *LIGO* 6/3/11

TMS Telescope Alignment

Michael Smith, Virginio Sannibale

Distribution of this document:
LIGO Scientific Collaboration

This is an internal working note
of the LIGO Laboratory.

California Institute of Technology
LIGO Project – MS 18-34
1200 E. California Blvd.
Pasadena, CA 91125
Phone (626) 395-2129
Fax (626) 304-9834
E-mail: info@ligo.caltech.edu

Massachusetts Institute of Technology
LIGO Project – NW22-295
185 Albany St
Cambridge, MA 02139
Phone (617) 253-4824
Fax (617) 253-7014
E-mail: info@ligo.mit.edu

LIGO Hanford Observatory
P.O. Box 159
Richland WA 99352
Phone 509-372-8106
Fax 509-372-8137

LIGO Livingston Observatory
P.O. Box 940
Livingston, LA 70754
Phone 225-686-3100
Fax 225-686-7189

http://www.ligo.caltech.edu/

1 Introduction 7

2 TMS Telescope Alignment Procedure 7

2.1 Support Bridge Adjustment 7

2.2 Secondary Mirror Mount Alignment 8

2.2.1 Lateral Alignment 8

2.2.2 Axial (Focus) Alignment 8

2.3 Telescope Alignment Preparation 8

2.3.1 ALIGN Autocollimator #1 8

2.4 Installation of Primary Mirror 9

2.5 Alignment of F1 and F2 10

2.6 Placement of the Shack-Hartmann/Autocollimator #3 Instrument 13

2.7 Alignment of the Shack-Hartmann/Autocollimator #3 Instrument 16

2.8 Single Pass Alignment 18

2.9 Double Pass Alignment 20

2.9.1 Aligning the Telescope Optical Axis with AC3 21

2.9.1.1 Current Method 21

2.9.1.2 Alternative Method (not done with the current alignment) 21

2.10 Shack-Hartmann Alignment of Telescope 21

2.10.1 Shack-Hartman Reference Data 22

2.10.1.1 Reference Beam View on Shack-Hartmann Sensor 22

2.10.1.2 Reference Sensor Line View 22

2.10.1.3 Reference Input Wavefront 23

2.10.1.4 Reference Zernike Coefficients 24

2.10.2 Double Pass Data 24

2.10.2.1 Double Pass Beam View on Shack-Hartmann Sensor 24

2.10.2.2 Double Pass Sensor Line View 25

2.10.2.3 Double Pass Input Wavefront 26

2.10.2.4 Double Pass Zernike Coefficients 26

3 Zemax Simulation 29

3.1 Initial Autocollimator Alignment 29

3.2 ZEMAX Interferometer Arm Cavity Beam Propagation Through Transmon System 33

3.3 ZEMAX Double Pass Alignment of TMS Telescope Using Shack-Hartmann Sensor 34

3.3.1 ETM HR Surrogate ... 34
3.3.2 Astigmatic Foci Displacement after Simulated Shack-Hartmann Alignment 41
3.3.2.1 Check of the IFO Beam Propagation with the ETM HR Surrogate Alignment ... 43
3.3.3 Alternate Flat Mirror Alignment ... 45
3.3.3.1 Check of the IFO Beam Propagation with the Flat Mirror Alignment . 49
3.3.4 Telescope Performance with Non-Gaussian Input Beams ... 51
3.3.5 ABCD Matrix Gaussian Beam Propagation ... 54
3.3.5.1 Gaussian Beam Propagation from IFO Beam Waist to 2ndary Mirror of TMS Telescope ... 54
3.3.5.2 Astigmatic Focus of TMS Telescope with Spherical Mirrors ... 55
4 Optical Aberration Theory ... 56
4.1 ZEMAX Zernike Coefficients ... 56
4.2 Shack-Hartmann Zernike Coefficients ... 57
4.3 Guoy Phase vs Astigmatic Focus Shift ... 57

Table of Figures

Figure 1: TMS Telescope Mounted Inside Support Bridge ... 7
Figure 2: Autocollimator #1 next to the TMS Telescope Input End ... 9
Figure 3: Primary Mirror Installation ... 10
Figure 4: Acetate Alignment Target on Surface of F2; Primary Alignment Mirror in Alignment Disk ... 11
Figure 5: Pitch and Yaw Adjustment of F1 ... 12
Figure 6: Pitch and Yaw Adjustment of F2 ... 13
Figure 7: Shack-Hartmann/Autocolllimator #3 Breadboard ... 14
Figure 8: Pedestal Translation and Tilt Adjustment ... 15
Figure 9: Pedestal Rotation Pivot ... 16
Figure 10: Retro Mirror to Measure Input Beam Wavefront ... 18
Figure 11: Installed 2ndary Mirror, Showing Cut-off Allen Wrench for Adjusting Vertical Translation of 2ndary Mirror Mount ... 18
Figure 12: Allen Wrench for Adjusting Axial Focus of 2ndary Mirror Mount ... 19
Figure 13: Allen Wrench for Adjusting Horizontal Translation of 2ndary Mirror Mount ... 20
Figure 14: Contour of the Input Beam on Shack-Hartmann Sensor ... 22
Figure 15: Reference Power Read by the Shack-Hartman Lens Array ... 23
Figure 16: Input Wavefront ... 23
Figure 17: Zernike Coefficients of the Input Beam ... 24
Figure 18: Contour of the Double Pass Beam ... 25
Figure 19: Power Read by the Shack-Hartman Lens Array after Double Pass ... 25
Figure 20: Return Wavefront after Double Pass ... 26
Figure 21: Double Pass Zernike Coefficients ... 27

Figure 22: Double Pass Reticle Pattern with Centered Shack-Hartmann Laser Beam... 28
Figure 23: Spot Diagram Showing the Two Astigmatic Foci after Initial Autocollimator Alignment ... 29
Figure 24: Left Shifted Focal Position of X-focus, after Initial Autocollimator Alignment ... 30
Figure 25: Right Shifted Focal Position of Y-focus, after Initial Autocollimator Alignment ... 30
Figure 26: Wavefront of Double Pass Output Beam at 2ndary Mirror, after Initial Autocollimator Alignment ... 31
Figure 27: Output Beam Profile at 2ndary Mirror. after Initial Autocollimator Alignment ... 32
Figure 28: Output Beam Phase at 2ndary Mirror, after Initial Autocollimator Alignment ... 33
Figure 29: IFO Beam Propagation Model from IFO Beam Waist through the Transmon Optical System. ... 34
Figure 30: ZEMAX Sequential Ray Trace of Double Pass through Telescope with ETM Surrogate Mirror ... 35
Figure 31: Input Beam Waist Cross Section at 2ndary Mirror, with ETM Surrogate Mirror ... 36
Figure 32: Phase of Input Beam Waist at 2ndary Mirror, with ETM Surrogate Mirror . 37
Figure 33: Cross Section of Output Beam at 2ndary Mirror, with ETM Surrogate Mirror ... 38
Figure 34: Phase of Output Beam at 2ndary Mirror, with ETM Surrogate Mirror... 39
Figure 35: Phase of Output Beam at Shack-Hartmann Sensor Location, with ETM Surrogate Mirror ... 39
Figure 36: Phase Map of Output Beam, with ETM Surrogate Mirror... 40
Figure 37: Spot Diagram Showing No Astigmatic Foci... 42
Figure 38: No Shift of X-focus... 42
Figure 39: No Shift of Y-focus ... 43
Figure 40: Cross Section of IFO Output Beam at 2ndary Mirror of Aligned Telescope, with ETM HR Surrogate ... 44
Figure 41: Phase of IFO Output Beam at 2ndary Mirror of Aligned Telescope, with ETM HR Surrogate ... 44
Figure 42: Optical Layout for Double Pass Flat Mirror Alignment... 46
Figure 43: Cross Section of Output Beam at 2ndary Mirror, with Flat Mirror... 47
Figure 44: Phase of Output Beam at 2ndary Mirror, with Flat Mirror... 47
Figure 45: Phase of Output Beam at Shack-Hartmann Sensor Location, with Flat Mirror ... 48
Figure 46: Contour of IFO Output Beam Cross Section at 2ndary Mirror, with Flat Mirror ... 50
Figure 47: Phase of IFO Output Beam at 2ndary Mirror, with Flat Mirror ... 50
Figure 48: Top Hat Input beam: Profile... 51
Figure 49: Top Hat Input beam: Phase... 52
Figure 50: Top Hat Output beam: Profile... 53
Figure 51: Top Hat Output beam: Phase ... 54
Figure 52: Guoy Phase vs Standard Zernike Astigmatism Coefficient ... 59

Abstract

Autocollimators and a Shack-Hartmann sensor are used to align the TMS Telescope. Two alignment methods are presented: alignment by double pass retro-reflection from a curved ETMHR surrogate mirror, and double pass retro-reflection from a flat mirror. A step-by-step procedure is presented, together with actual data from the Shack-Hartmann sensor during the alignment procedure. Optical aberration theory is used to derive a relationship between the Zernike astigmatic coefficient and the Guoy phase error at the focal plane of the TMS sensing system. The ZEMAX focus parameters for an ideal off-axis parabolic telescope agree with the ABCD Gaussian beam propagation calculations.

1 Introduction

Autocollimators and a Shack-Hartmann sensor are used to align the TMS Telescope. Two alignment methods are presented: alignment by double pass retro-reflection from a curved ETMHR surrogate mirror, and double pass retro-reflection from a flat mirror. A step-by-step procedure is presented, together with actual data from the Shack-Hartmann sensor during the alignment procedure. Optical aberration theory is used to derive a relationship between the Zernike astigmatic coefficient and the Guoy phase error at the focal plane of the TMS sensing system. The ZEMAX focus parameters for an ideal off-axis parabolic telescope agree with the ABCD Gaussian beam propagation calculation.

2 TMS Telescope Alignment Procedure

2.1 Support Bridge Adjustment

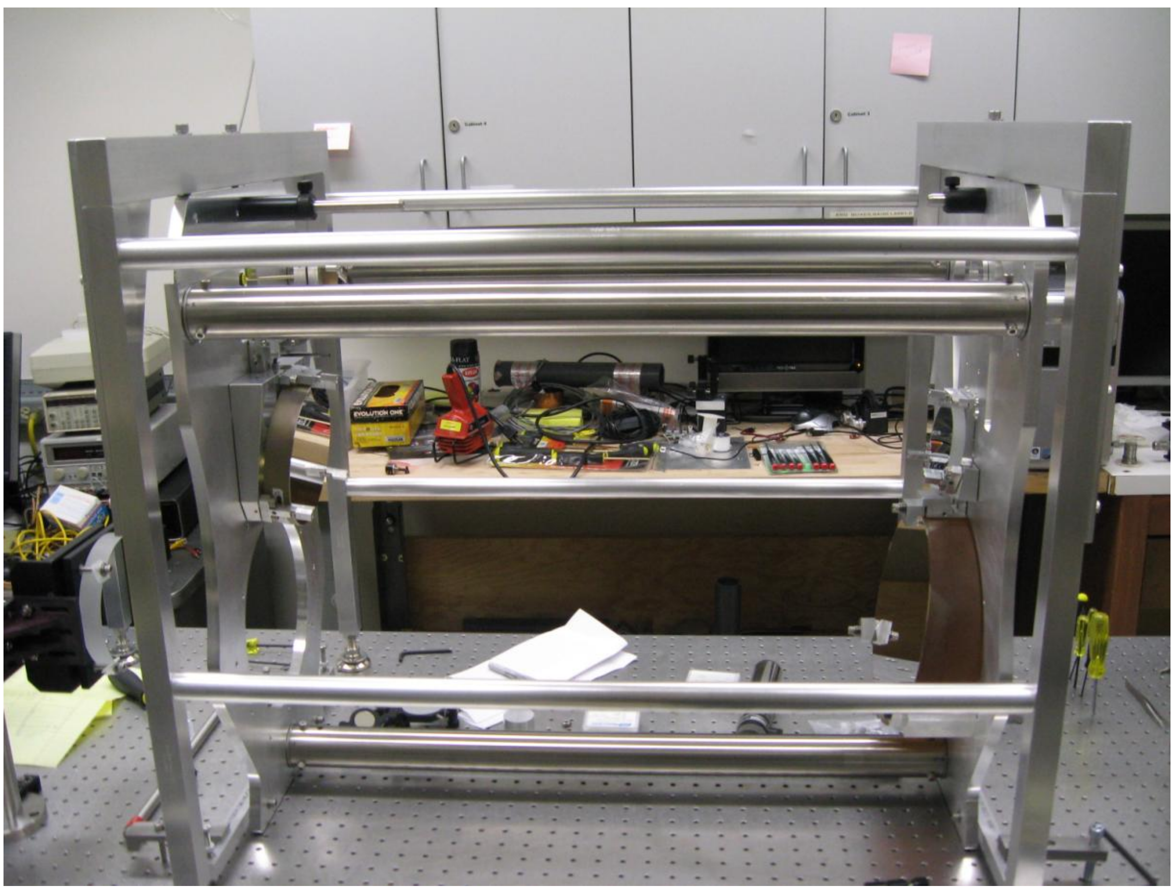

Figure 1: TMS Telescope Mounted Inside Support Bridge

- Loosen the attachment bolts and lower the Telescope in the support bridge until the 3 pads at the bottom of the Telescope touch the table, without any tension on the 3 support screws attached to the support frame.
- Advance the bolts on the four corners of the outrigger bars until they touch the table
- Clamp the outrigger bars to table using appropriate clamps

2.2 Secondary Mirror Mount Alignment

2.2.1 Lateral Alignment

- Attach the autocollimator holder in the back plate of the TMS telescope. Use the cylindrical bushing to center the holder within the hole in the plate.
- Insert autocollimator #2 (AC2) in the holder.
- Insert a 1.5 inch parallel mirror (window) into the 2ndary mirror mount—press it against the three back pads using screws and washers.
- Focus AC2 to infinity. Pitch and yaw the 2ndary mirror mount to center the reticle pattern in AC2.
- Take out the 1.5 in mirror and insert the metal 2ndary alignment plug, holding the plug in place with the set screw in the mirror mount.
- Focus and sight on the cross pattern of the alignment plug with AC2; move the 2ndary mirror mount vertically and horizontally to center the cross pattern with the cross hairs of AC2.

2.2.2 Axial (Focus) Alignment

- Remove the autocollimator holder and place a 0.25 thick mirror against the mounting pads of the autocollimator holder in the inside face of the telescope back plate. The mirror faces toward the outside of the telescope.
- Use the focus gauge rod to set the distance between the 2ndary mirror metal alignment plug and the back of the mirror—adjust the focus screw on the 2ndary mirror mount until the gauge rod touches both the metal alignment plug and the back of the mirror.

2.3 Telescope Alignment Preparation

2.3.1 ALIGN Autocollimator #1

- Place the mount for autocollimator #1 (AC1) on the Newport Table next to the TMS telescope input end, leaving room to later place the Retro Mirror between AC1 and the Telescope.

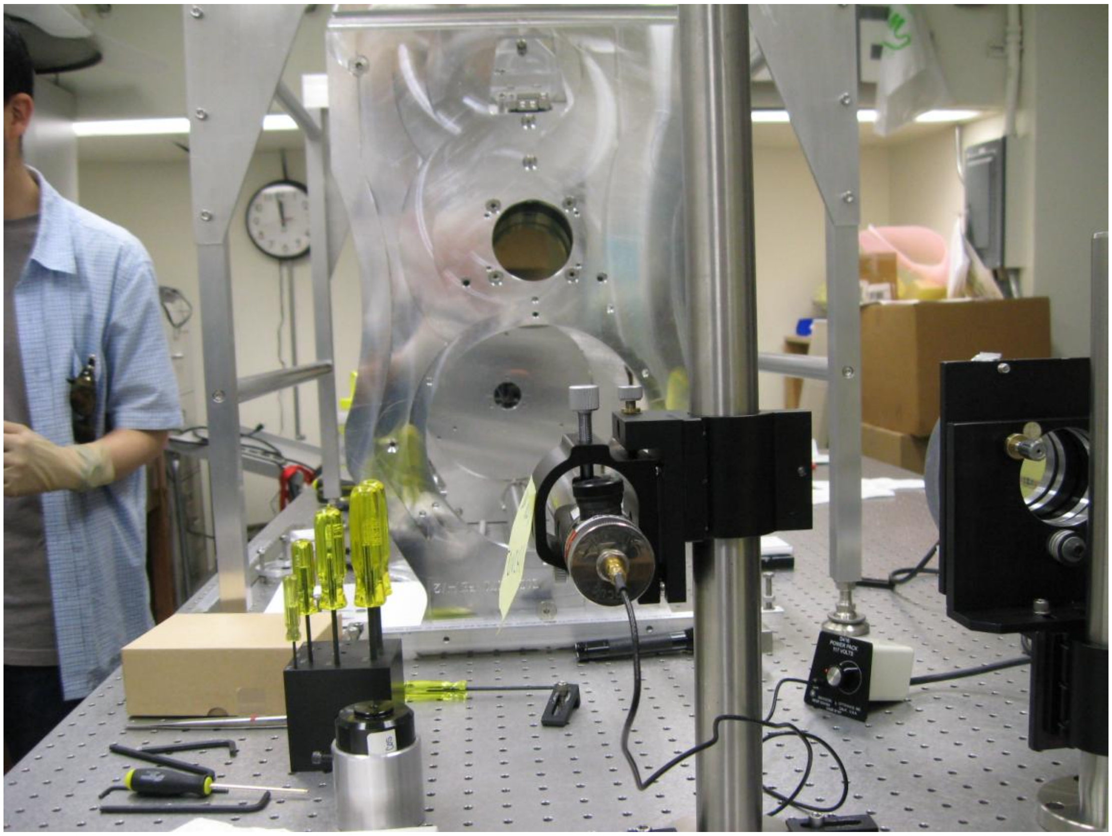

Figure 2: Autocollimator #1 next to the TMS Telescope Input End

- Attach the 2" dia mirror primary alignment mirror in the primary alignment disk using the ring clamp. Mount the disk against the primary mirror mounting pads in the back plate of the telescope; the cross pattern on the disc should be oriented in a nominal horizontal and vertical direction. See Figure 4.
- Retro-reflect the AC1 beam from the primary alignment mirror and adjust pitch and yaw of AC1 to center the reticle pattern on the cross hairs of AC1.
- Focus AC1 on the cross scribed on the disk and translate AC1 horizontally and vertically until the cross hair of AC1 is aligned with the cross on the disk.
- Iterate between translating AC1 and retro reflecting from the alignment mirror until AC1 is both centered and perpendicular to the primary alignment mirror. **AC1 is now aligned and defines the input optical axis of the telescope...do not move AC1!!**
- Need to order vertical and horizontal slides for AC1.
- Need spring to remove backlash of 2ndary vertical slide
- Need closure spring for 2ndary mount pitch and yaw

2.4 Installation of Primary Mirror

- Remove the primary mount alignment mirror, and install the primary mirror; the mark on the thin side of the mirror must align with the vertical mark on the top mounting pad for the primary mirror.

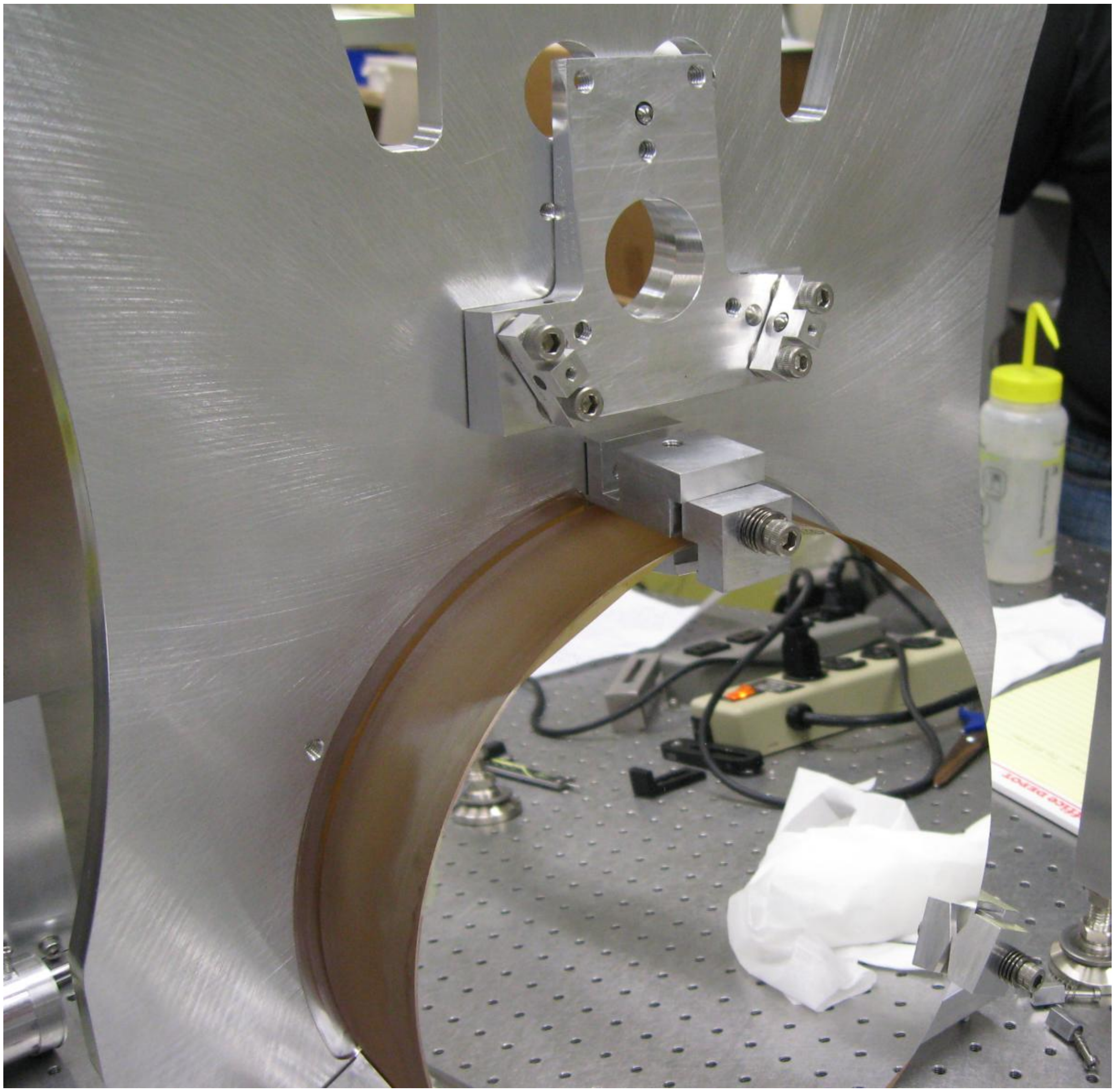

Figure 3: Primary Mirror Installation

2.5 Alignment of F1 and F2

- Install fold mirrors F1 and F2
- Install the 2ndary alignment plug into the 2ndary mirror mount
- Place and hold the acetate target against the surface of F2 using spring clips; center the target with the diameter of F2 mirror, and orient the cross pattern approximately horizontally and vertically.

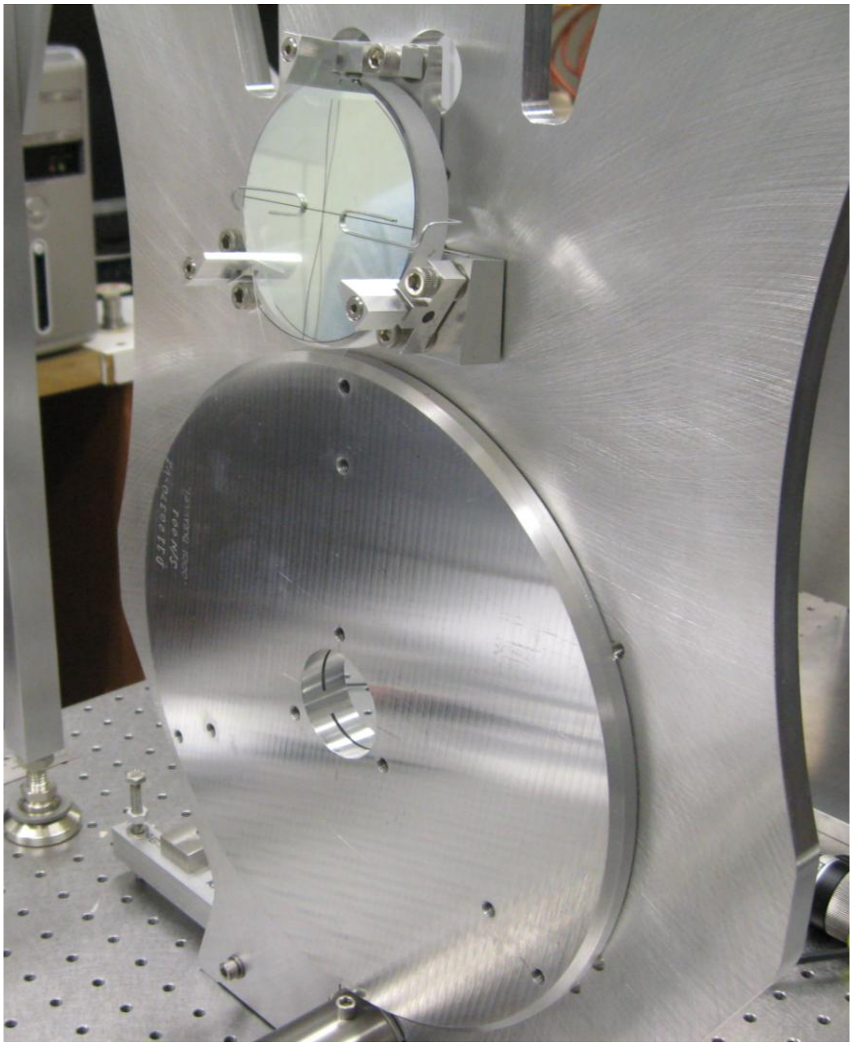

Figure 4: Acetate Alignment Target on Surface of F2; Primary Alignment Mirror in Alignment Disk

- Adjust the focus of AC1 to sight the cross pattern on the F2 target.
- Adjust the pitch and yaw of F1 until the cross pattern on F2 is centered with the cross hairs of AC1.

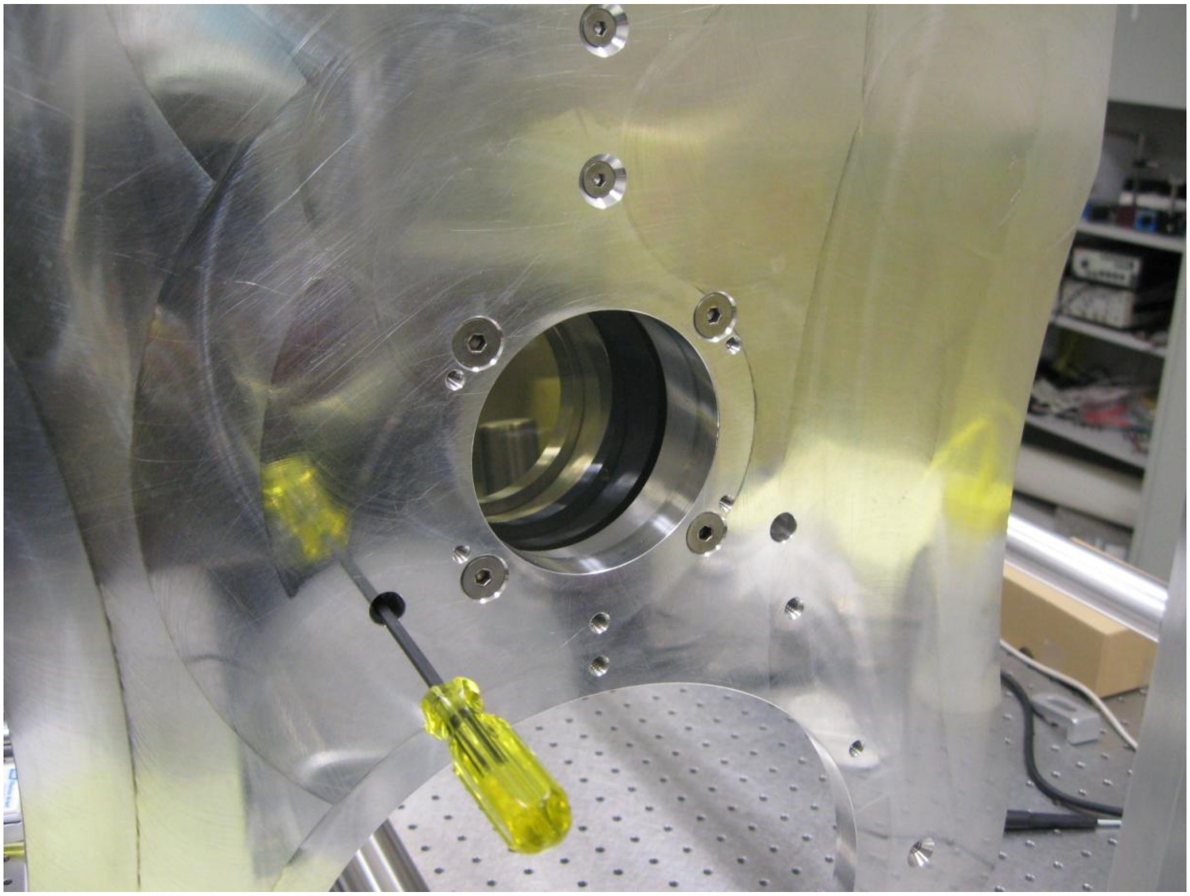

Figure 5: Pitch and Yaw Adjustment of F1

- Adjust the focus of AC1 to sight the cross pattern on the 2ndary alignment plug.
- Adjust the pitch and yaw of F2 until the cross pattern on the 2ndary alignment plug is centered with the cross hairs of AC1.

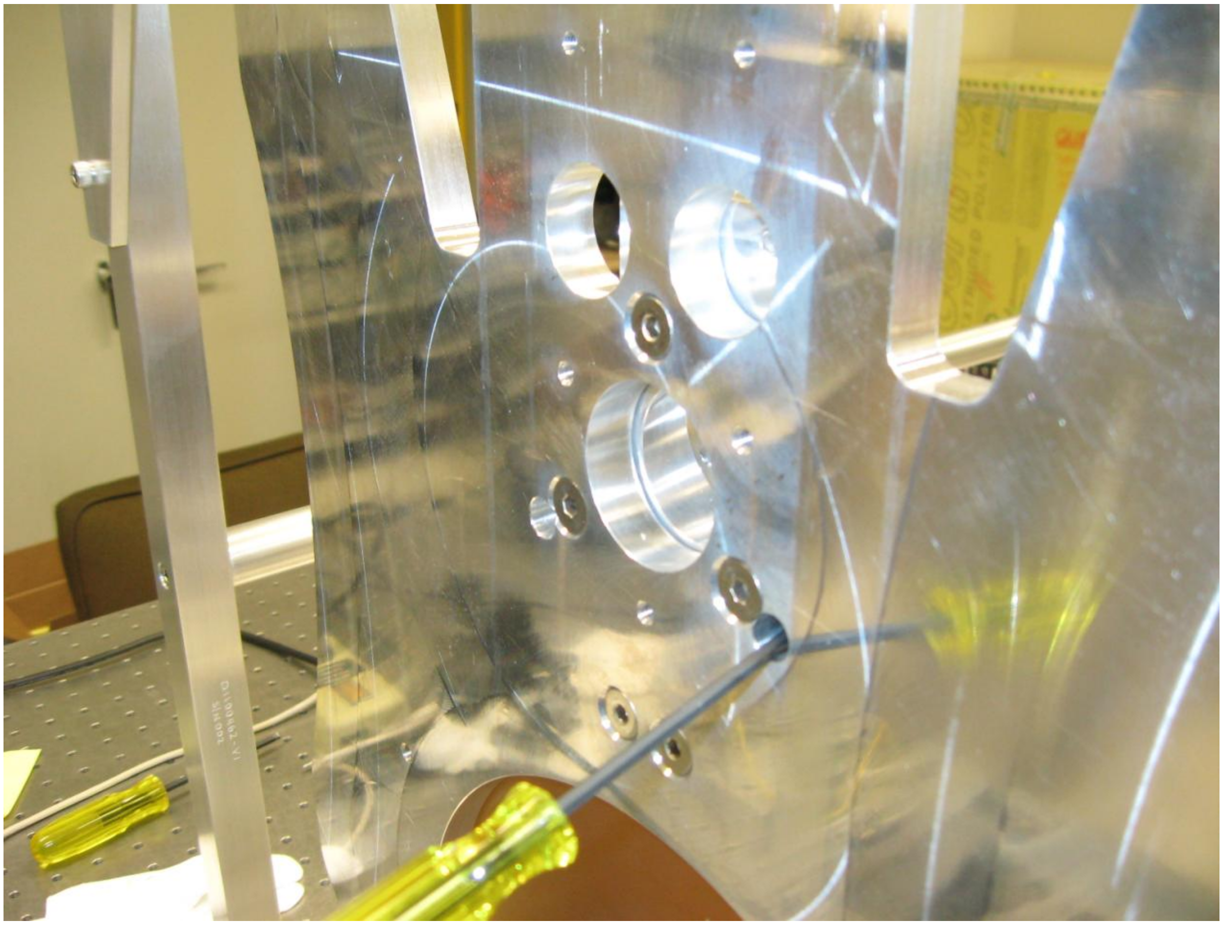

Figure 6: Pitch and Yaw Adjustment of F2

- When done, cross lock F1 and F2 with locking screws at 90 deg (see assembly drawing for location).

2.6 Placement of the Shack-Hartmann/Autocollimator #3 Instrument

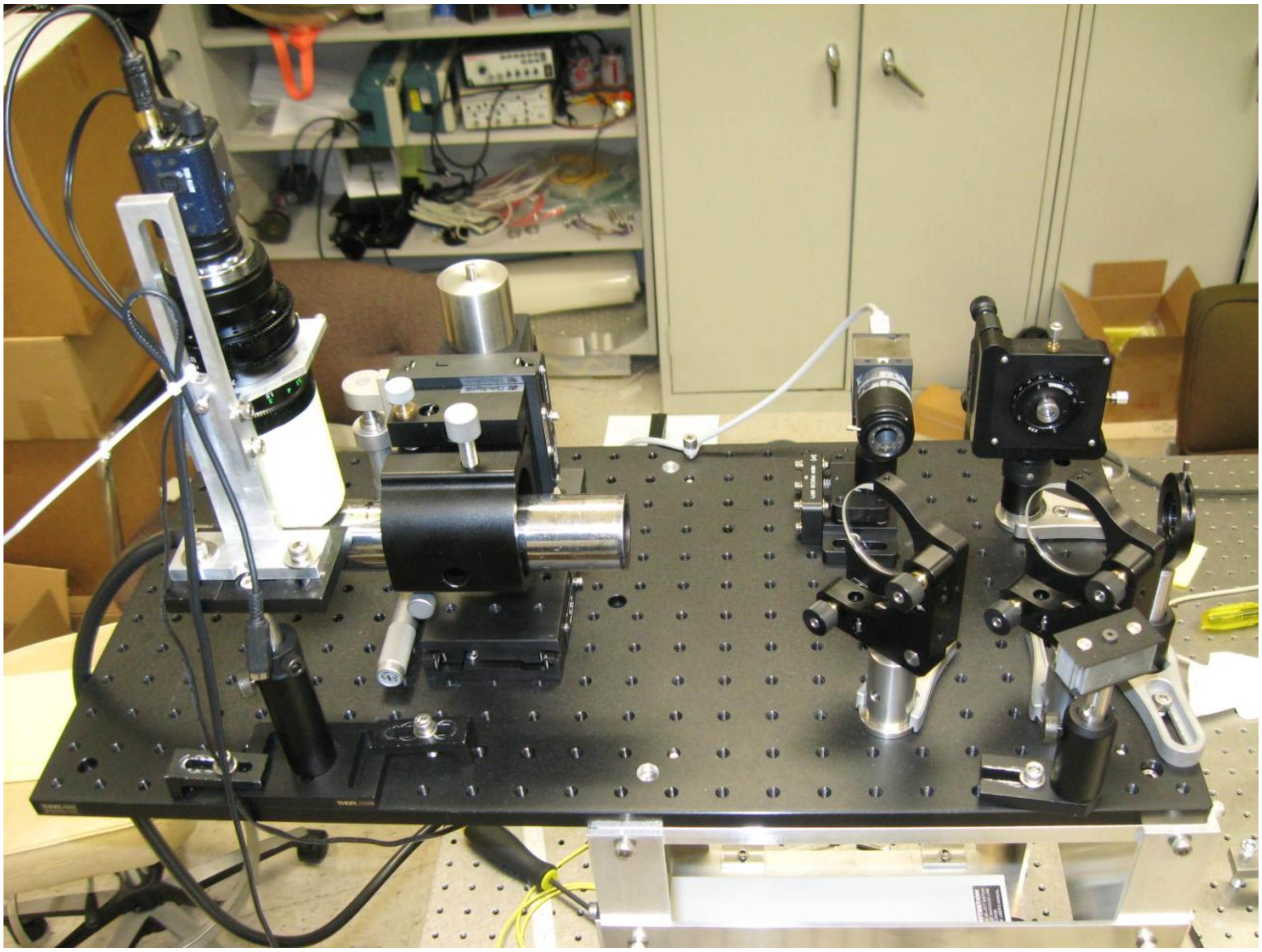

Figure 7: Shack-Hartmann/Autocolllimator #3 Breadboard

- Mount the Shack-Hartmann/Autocollimator #3 breadboard assembly to the top of the 18 in high mounting pedestal; set the front edge of the breadboard 11.5 inches away from the back surface of the back plate of the Telescope; this location places the S. H. sensor at the same distance to the S. H. reference mirror as the distance from the S. H. reference mirror to the 2ndary mirror, so that when a reference beam waist is set during the initial alignment of the S. H. this beam waist will also occur at the 2ndary mirror.
- Move the pedestal until AC3 centerline in approximately centered and perpendicular to the back plate of the telescope.

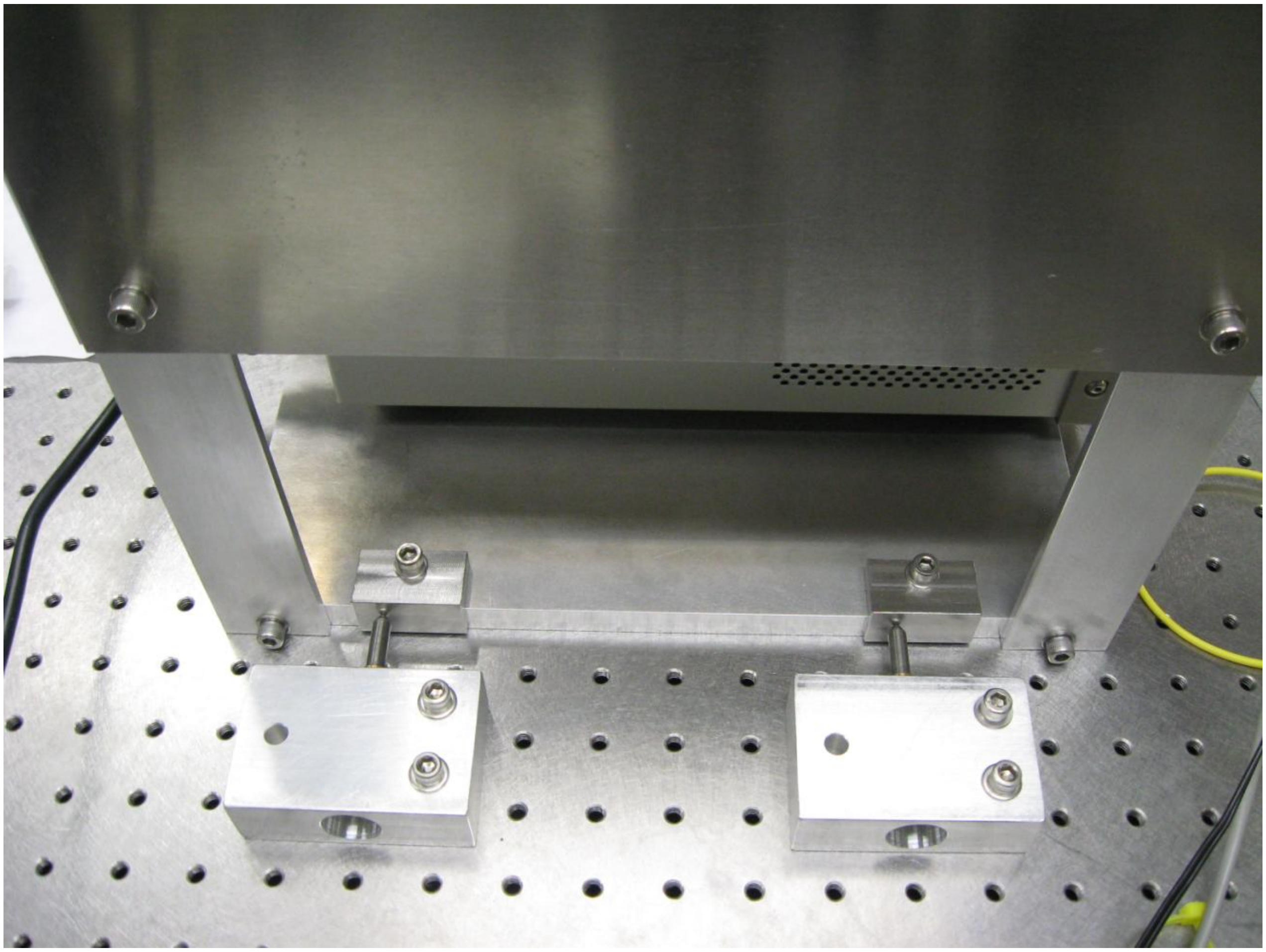

Figure 8: Pedestal Translation and Tilt Adjustment

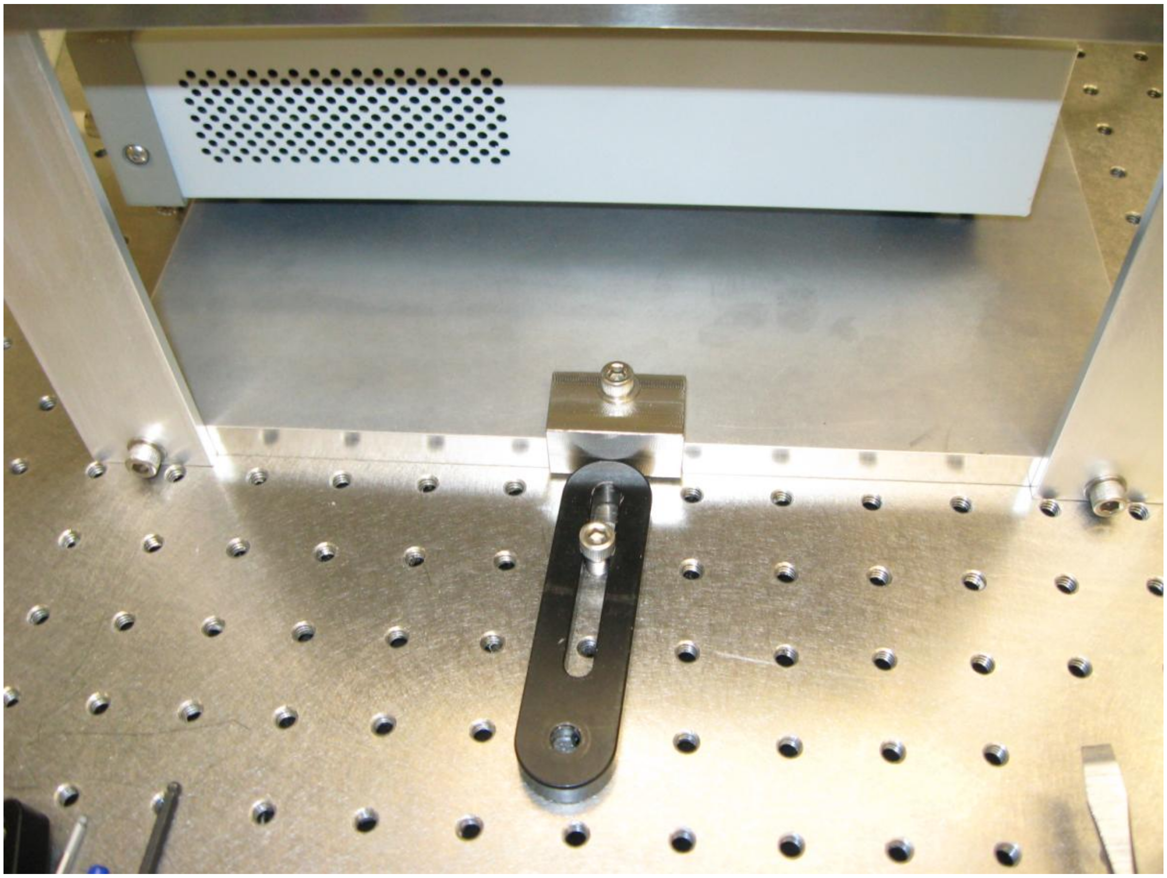

Figure 9: Pedestal Rotation Pivot

- Place a flat S. H. reference mirror against the mounting pads of the autocollimator holder to retroreflect the AC3 reticle pattern. Align the reticle pattern in the horizontal direction to the AC3 cross hairs by tilting the base of the pedestal with the pushing screws. The final alignment of AC3 is done by pitching and yawing AC3 within its mount.
- Remove the reference mirror and focus on the cross pattern on the 2ndary alignment plug with AC3; shift the base of the pedestal with the pushing screws until the AC3 cross hairs are centered horizontally with the 2ndary alignment plug. Raise AC3 until the cross hairs are centered vertically.
- Iterate between aligning AC3 horizontally and vertically to the 2ndary alignment plug, and aligning AC3 perpendicular to the reference mirror.

2.7 Alignment of the Shack-Hartmann/Autocollimator #3 Instrument

- Mount the S. H. reference mirror against the mounting pads of the autocollimator holder (see Figure 10; the 2 inch reference mirror was too small to fit on the pads, and instead, it was temporarily mounted as shown.)
- Raise the height of the laser source, the Shack-Hartmann detector, and the iris to the same height as the aligned AC3 on the breadboard.

- Pitch, yaw, and translate the laser collimating lens to align the laser beam co-linear with AC3 by observing the returned laser spot centered on the cross hairs of AC3, and by observing the alignment of the laser beam with the iris center.
- Translate the Shack-Hartmann detector and steer the beam splitter until the observed wavefront is centered and perpendicular to the Shack-Hartmann detector.
- Adjust the focus of the laser collimator until a minimum spot is obtained with the returned laser beam. (note: When this was done with the adjustable collimator, it was discovered that the beam waist radius was only 0.3 mm. In the future, a 10X beam expanding telescope should be added to the Shack-Hartmann apparatus to increase the beam waist to 3 mm radius.) This procedure sets the beam waist of the reference beam at the Shack-Hartmann detector. The distance from the Shack-Hartmann detector to the reference mirror is 23.5 inches; when the reference mirror is removed, the input beam waist for the telescope Shack-Hartmann alignment will be located 23.5 inches from the inside of the back plate toward the 2ndary mirror, which is close to the 2ndary mirror.
- Place a flat retro-mirror at this position to retro-reflect the beam back into the Shack-Hartmann sensor and record the Zernike coefficient; **these reference values will be subtracted from the Zernike readings when the telescope is aligned using the S. H.**

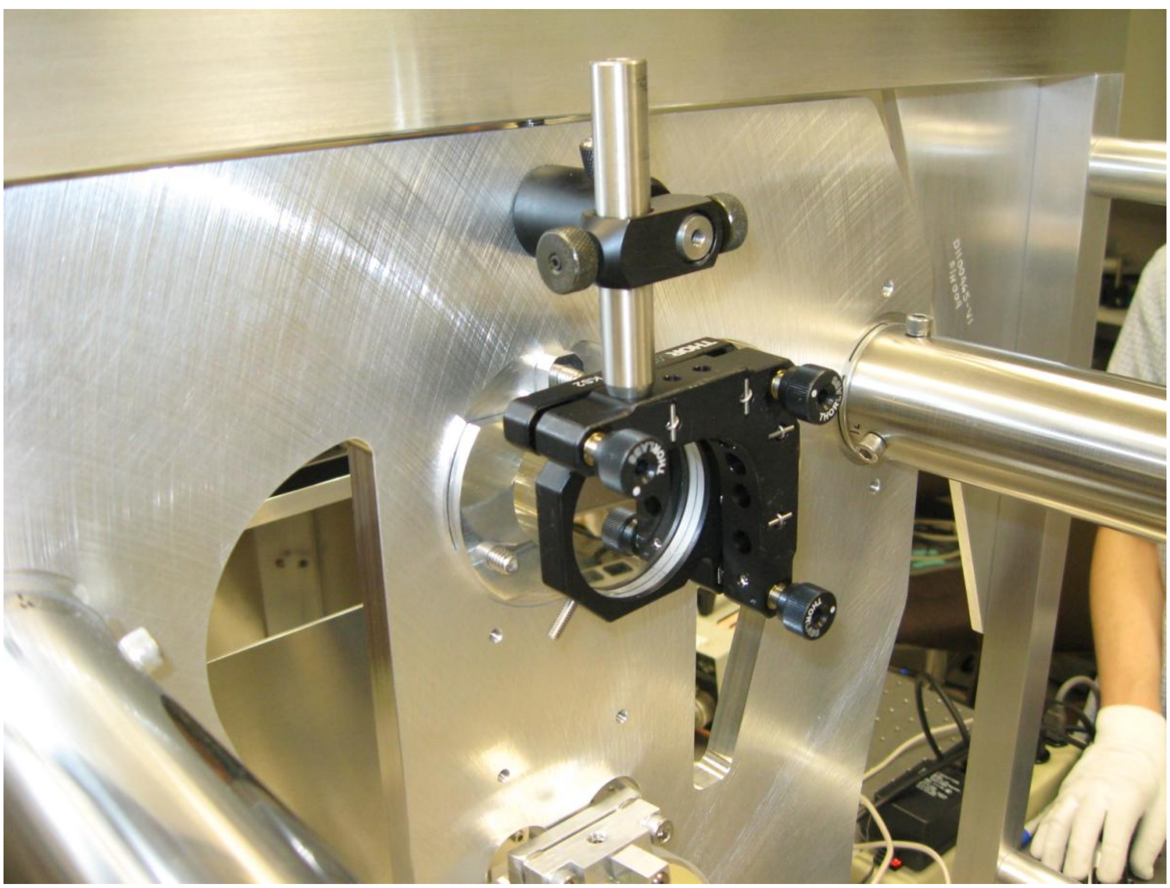

Figure 10: Retro Mirror to Measure Input Beam Wavefront

2.8 Single Pass Alignment

- Remove the 2ndary mirror mount alignment plug and install the secondary mirror; the thick side of the secondary mirror must align with the mark scribed on the top edge of the secondary mirror mount.

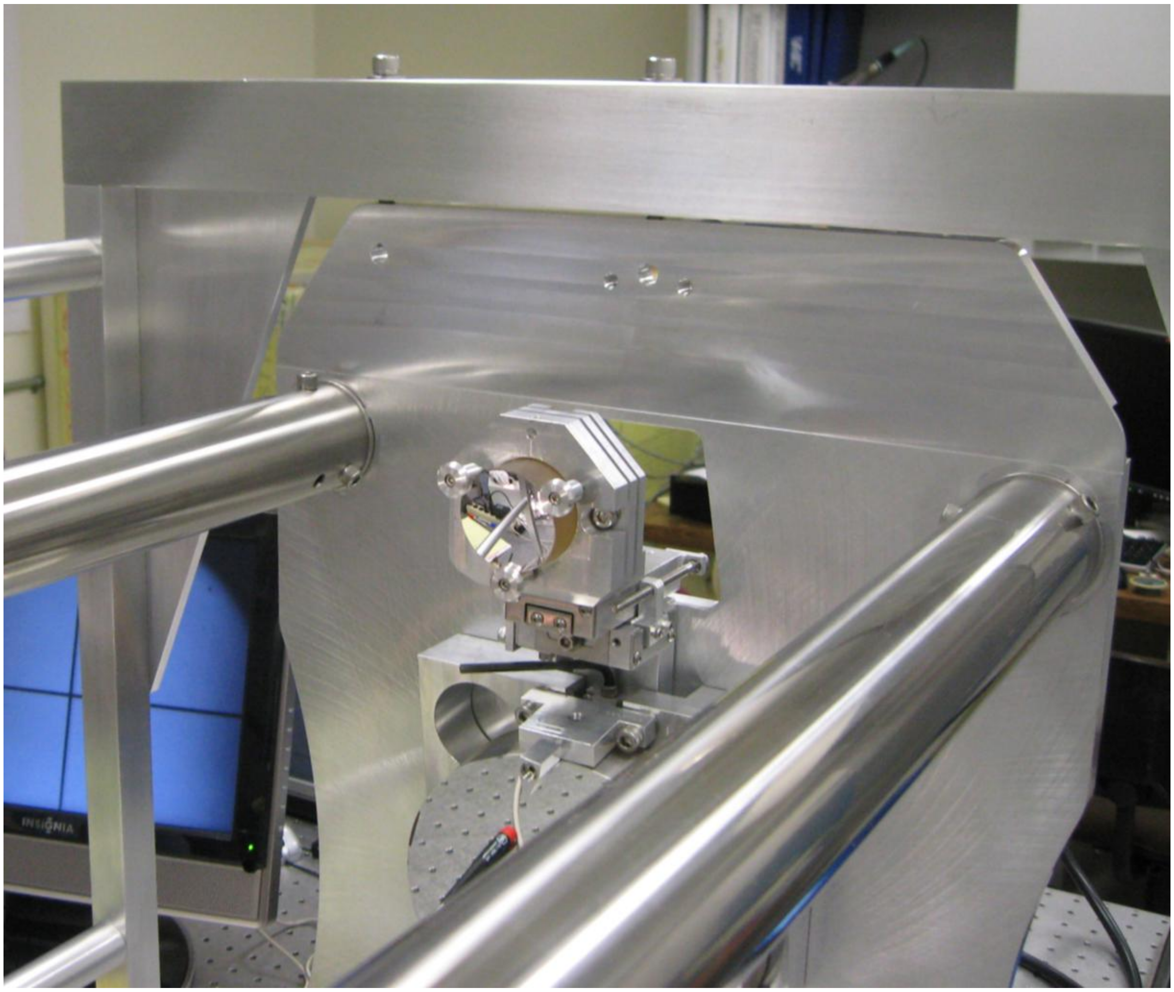

Figure 11: Installed 2ndary Mirror, Showing Cut-off Allen Wrench for Adjusting Vertical Translation of 2ndary Mirror Mount

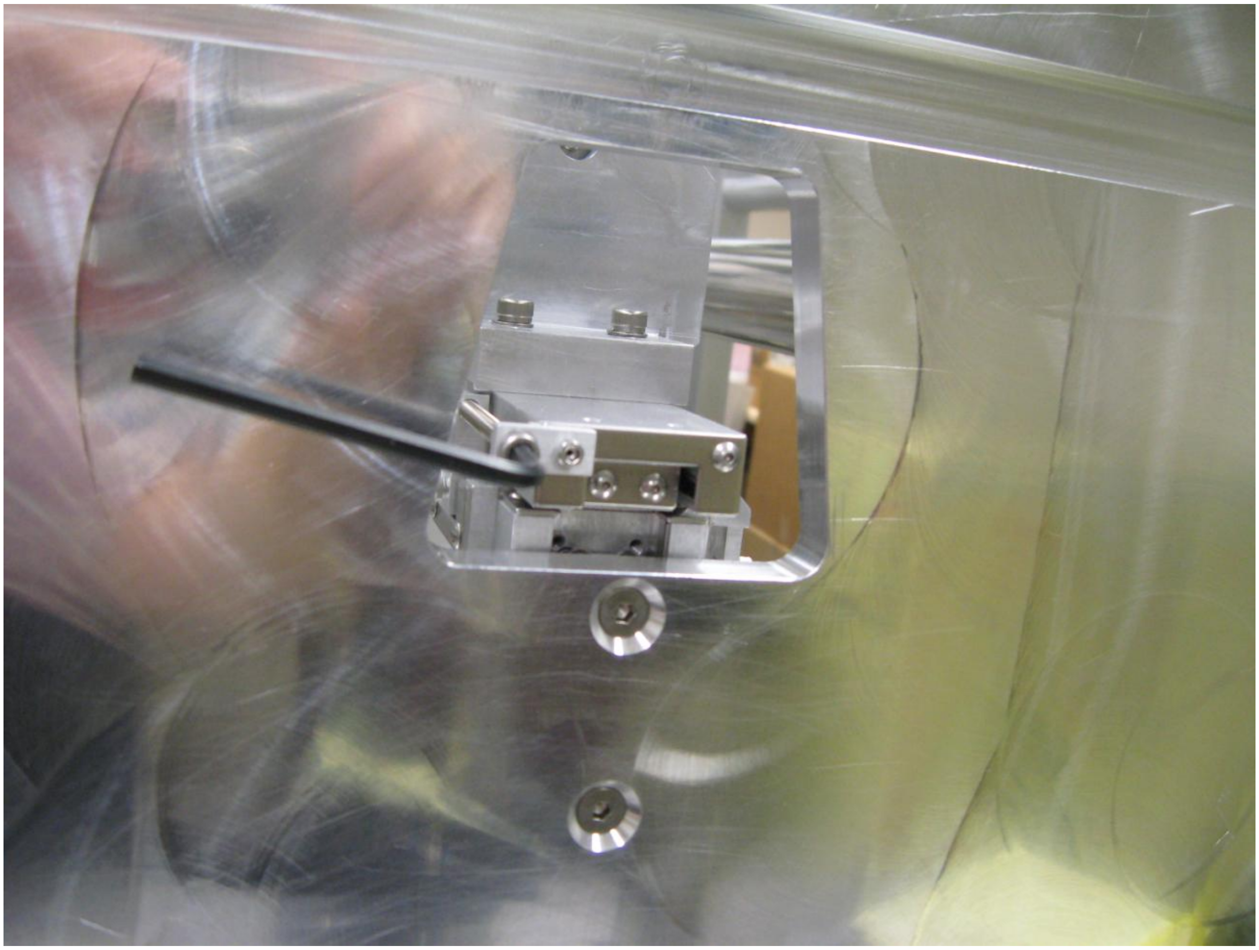

Figure 12: Allen Wrench for Adjusting Axial Focus of 2ndary Mirror Mount

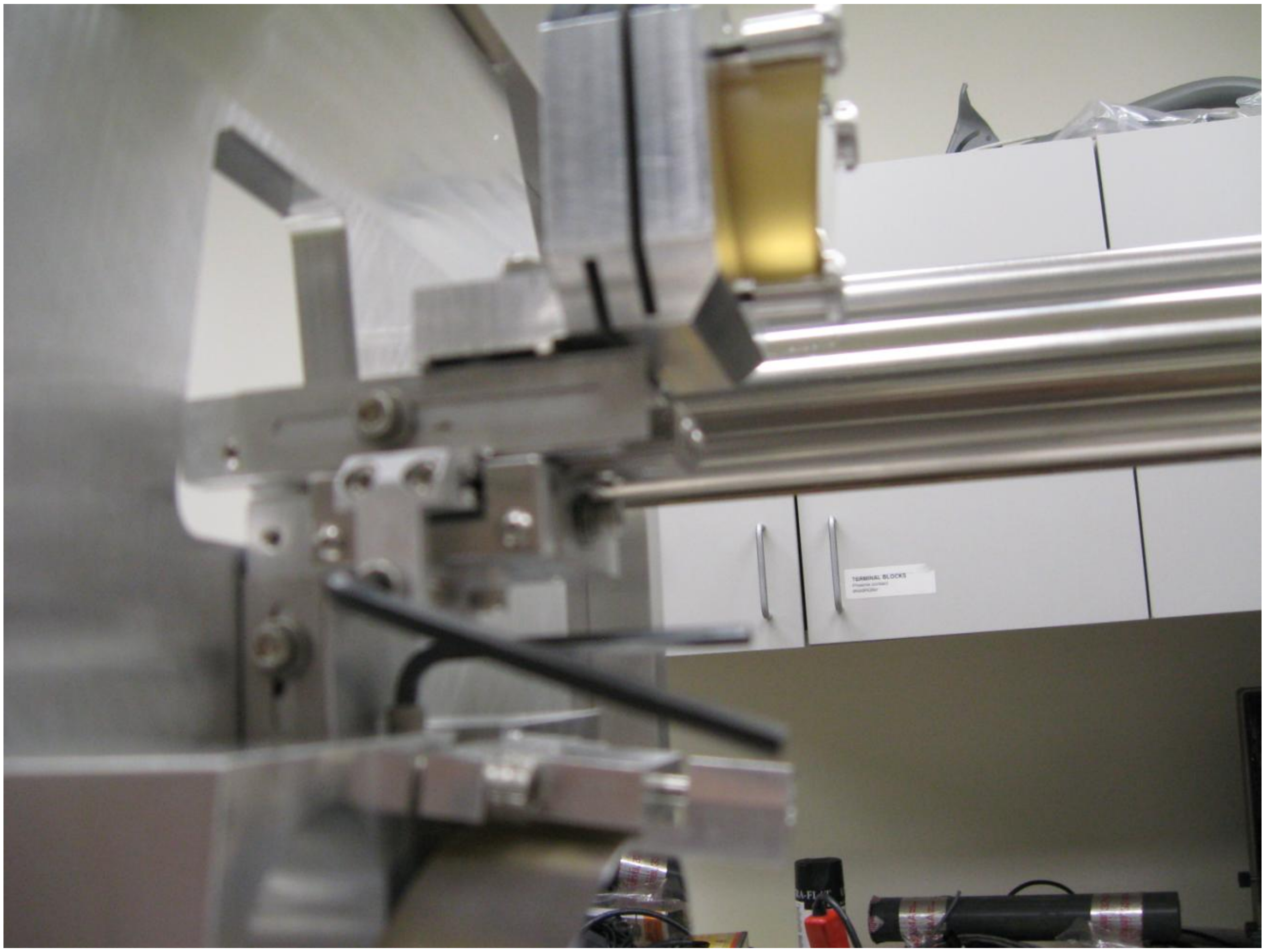

Figure 13: Allen Wrench for Adjusting Horizontal Translation of 2ndary Mirror Mount

- Turn on AC1 and focus at infinity
- Translate (do not tilt!) and focus the secondary mirror until the reticle pattern from AC1 in observed in AC3; continue to adjust the translation and focus of the secondary mirror until the reticle pattern in centered and sharply in focus in AC3.

2.9 Double Pass Alignment

- Place a 2245 meter radius of curvature, 25 mm thick, 6 in diameter mirror in a steerable mirror mount in front of the telescope input side between the telescope front plate and AC1, with the reflecting side away from the telescope. (For the current alignment, a 6 in lambda/10 flat mirror was used, which does not properly represent the ETM mirror focus condition.)
- Turn on AC3, and steer the 6 in mirror until the retro-reflected reticle pattern is visible in AC3, after a double pass through the telescope.
- Adjust the focus and the translation of the secondary mirror iteratively until the reticle pattern is centered and sharply focused in AC3.

- Autocollimate from the HR side of the 6 in mirror with AC1, and tilt the 6 in mirror while re-adjusting the translation and focus of the secondary mirror to keep the pattern sharp and centered in AC3. Continue this until the 6 in mirror is perpendicular to the AC1 beam.

2.9.1 Aligning the Telescope Optical Axis with AC3

2.9.1.1 Current Method

- Place a paper target at the input end of the telescope centered with the input aperture (in the future, we will have scribed marks in the horizontal and vertical axes on the inside of the entrance aperture plate.) Focus AC3 and project the reticle pattern onto the target; it will probably be observed that the reticle pattern is not centered with the target.
- Change the height of AC3, without disturbing the alignment of AC3 or the telescope until the projected reticle pattern in centered on the target.
- Realign the Shack-Hartmann sensor apparatus to match the new height of AC3.

2.9.1.2 Alternative Method (not done with the current alignment)

- Place a paper target at the input end of the telescope centered with the input aperture (in the future, we will have scribed marks in the horizontal and vertical axes on the inside of the entrance aperture plate.) Focus AC3 and project the reticle pattern onto the target; it will probably be observed that the reticle pattern is not centered with the target.
- Pitch F2, while compensating by translating the 2ndary mirror vertically, until the projected reticle pattern is centered with the target at the entrance aperture of the telescope. This may cause astigmatism, and the 2ndary mirror may have to be ajusted to remove the astigmatism by following the steps described in 2.10.

2.10 Shack-Hartmann Alignment of Telescope

- Reduce the Zernike coefficients Z4 and Z6, as displayed on the Shack-Hartmann screen, to minimum values by adjusting the horizontal and vertical pairs of coupled alignment adjustments of the 2ndary mirror mount: e.g. translate the mirror vertically, and compensate by pitching the mirror in order to return the laser beam to the center of the cross hairs of AC3; translate the mirror horizontally, and compensate by yawing the mirror in order to return the laser beam to the center of the cross hairs of AC3.

- Move the mirror axially to adjust the focus in order to minimize the defocus Zernike coefficient (Z5).

- After all adjustments of the 2ndary mirror mount are completed, lock down the secondary mirror mount with the locking plates

2.10.1 Shack-Hartman Reference Data

2.10.1.1 Reference Beam View on Shack-Hartmann Sensor

The input beam to the telescope was characterized by reflecting the input back to the Shack-Hartmann sensor by means of a lambda/10 mirror, as described in 2.7. The beam contour on the S. H. sensor is shown in Figure 14.

When the input beam was collimated to a beam waist at the input, the beam diameter was too small to be measured reliably with the Shack-Hartmann sensor. Therefore, the input beam was intentionally allowed to expand to a spherical beam at the input of the telescope. With this input beam, it was possible to adjust the telescope to remove the astigmatism and create a beam waist at the 2ndary mirror after a double pass; however, the telescope is not properly focused under these conditions.

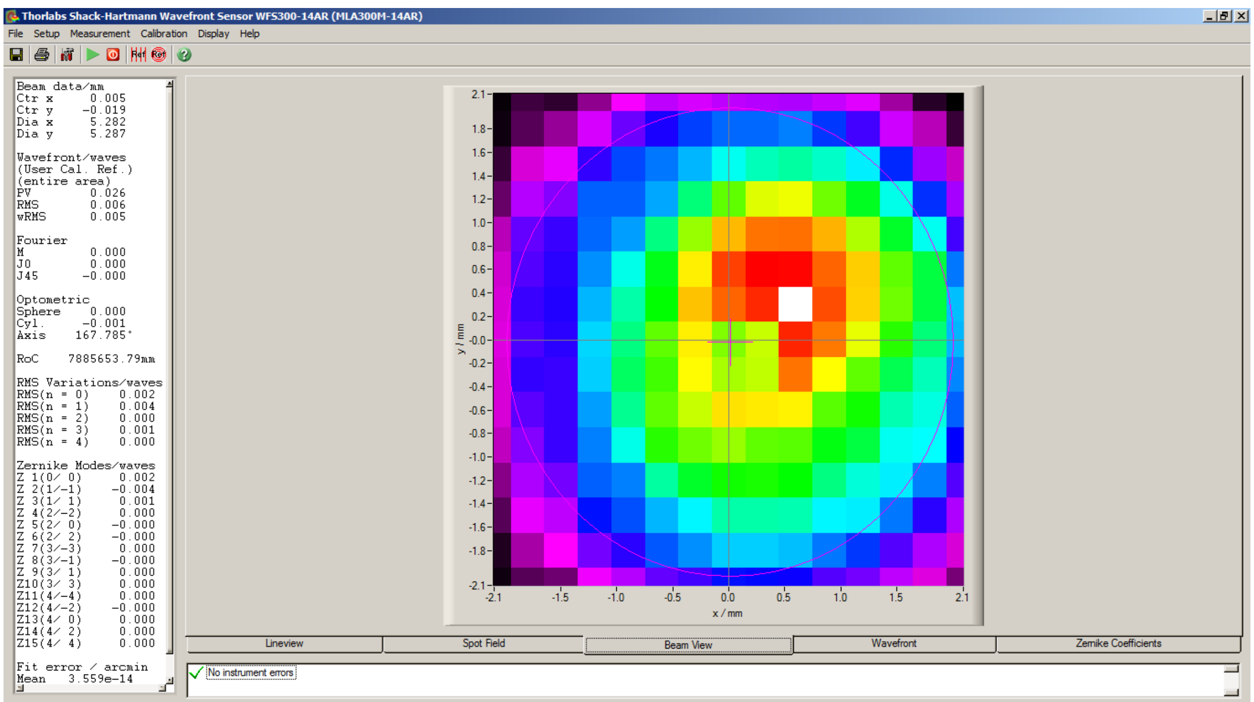

Figure 14: Contour of the Input Beam on Shack-Hartmann Sensor

2.10.1.2 Reference Sensor Line View

The power measured by the central array of the S. H. lens detector matrix is shown in Figure 15.

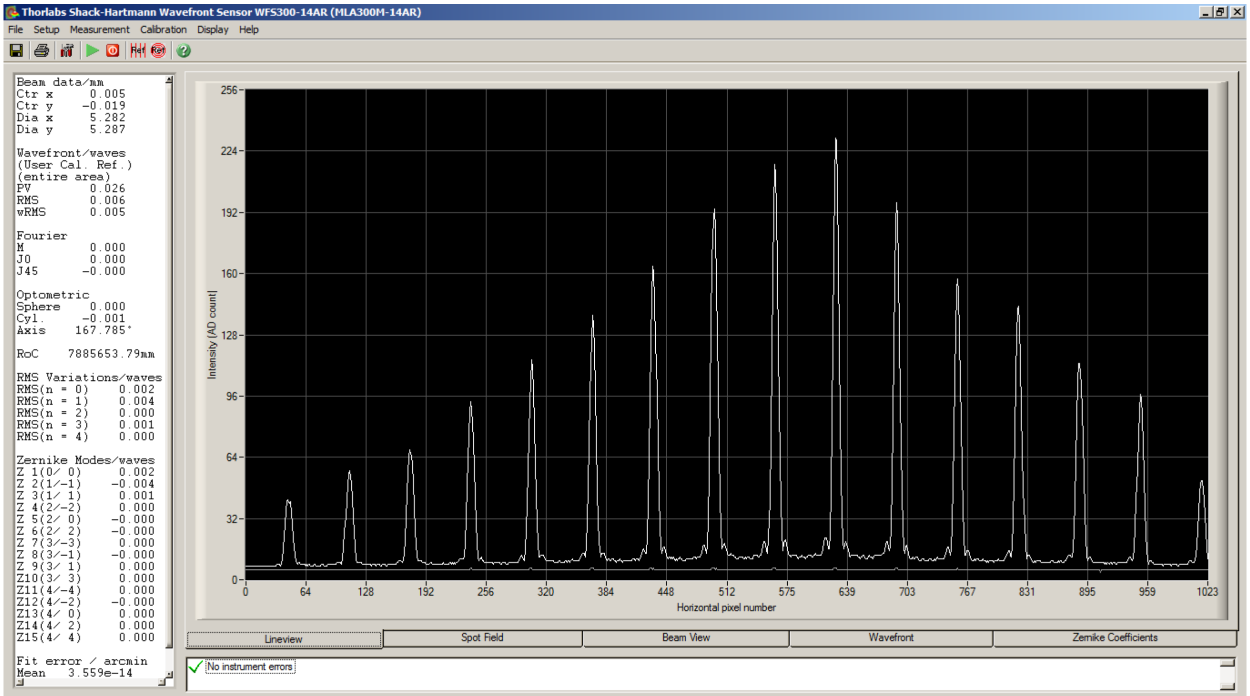

Figure 15: Reference Power Read by the Shack-Hartman Lens Array

2.10.1.3 Reference Input Wavefront

The reconstructed wavefront of the reference beam is shown in Figure 16. The curvature is 7.8 km, as measured by the Shack-Hartmann sensor, and the astigmatism is < one order of magnitude lower than the requirement 0.02 waves @ 1064 nm.

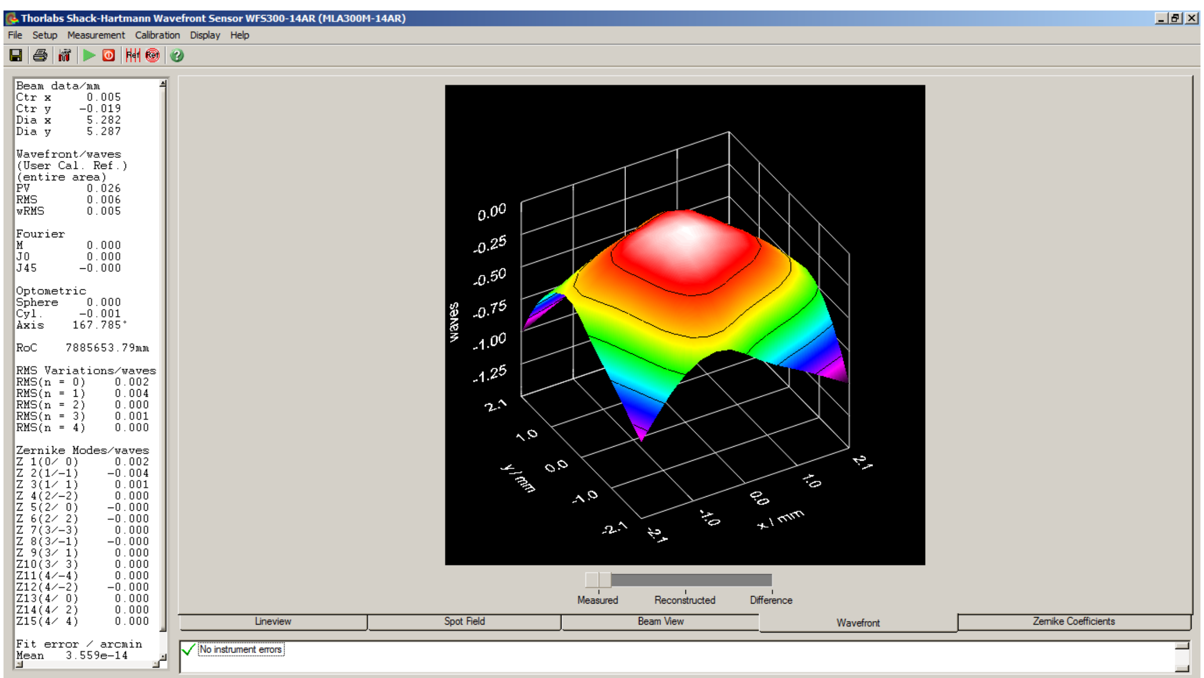

Figure 16: Input Wavefront

2.10.1.4 Reference Zernike Coefficients

The 1st 15 Zernike coefficients for the reference beam are shown in Figure 17.

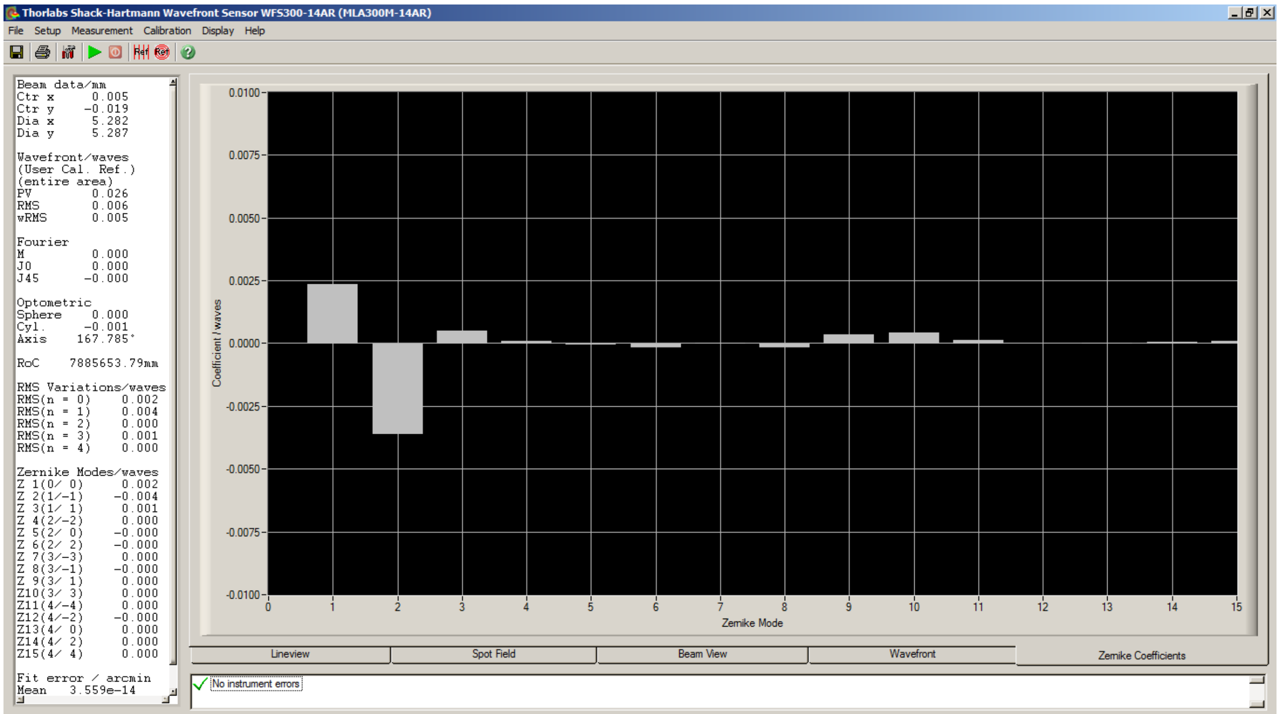

Figure 17: Zernike Coefficients of the Input Beam

2.10.2 Double Pass Data

The following screen shots show the data taken after the aligned double pass through the telescope. The reference data was subtracted to obtain these results.

2.10.2.1 Double Pass Beam View on Shack-Hartmann Sensor

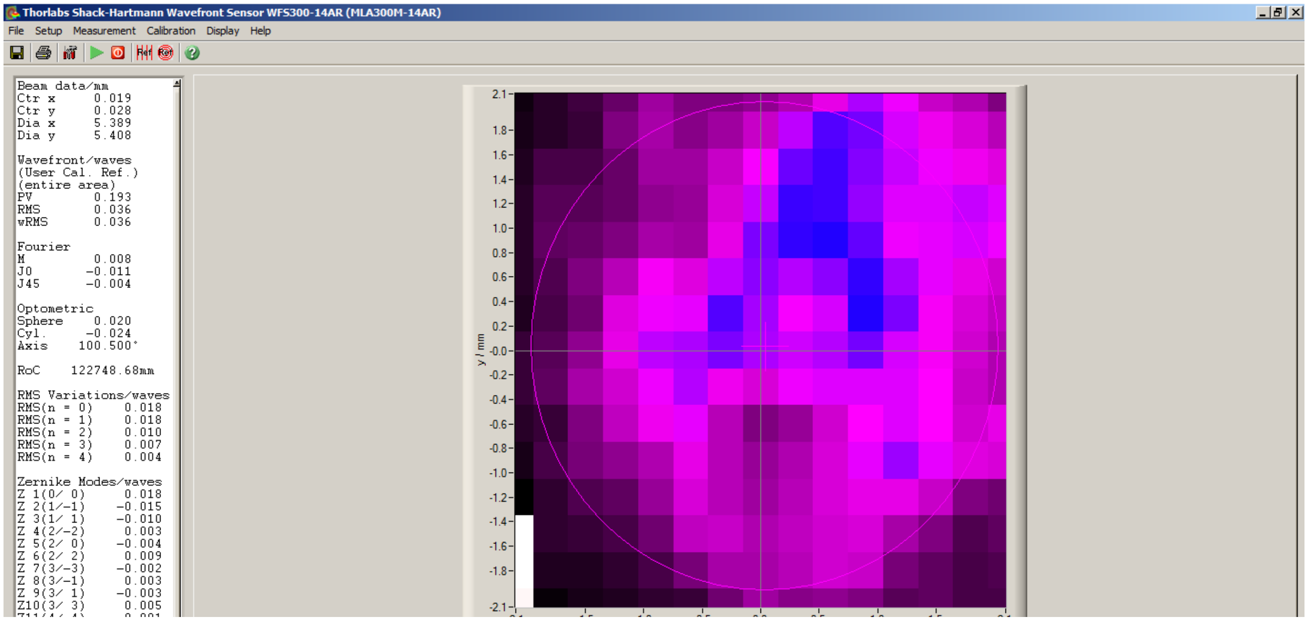

Figure 18: Contour of the Double Pass Beam

2.10.2.2 Double Pass Sensor Line View

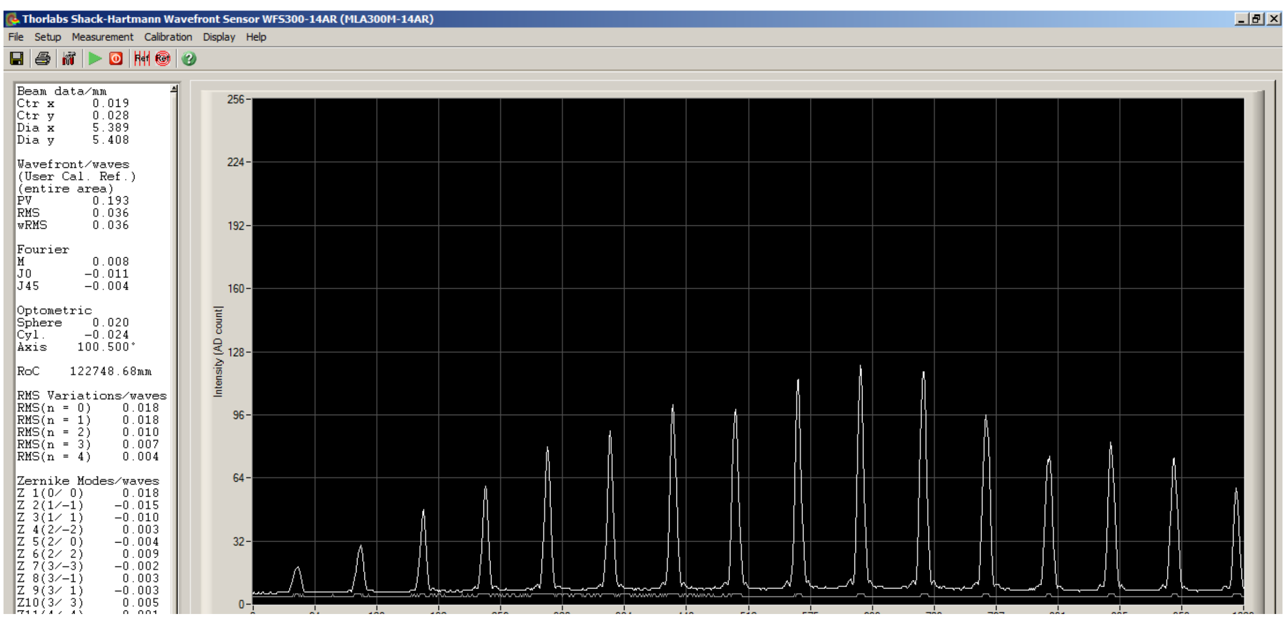

Figure 19: Power Read by the Shack-Hartman Lens Array after Double Pass

2.10.2.3 Double Pass Input Wavefront

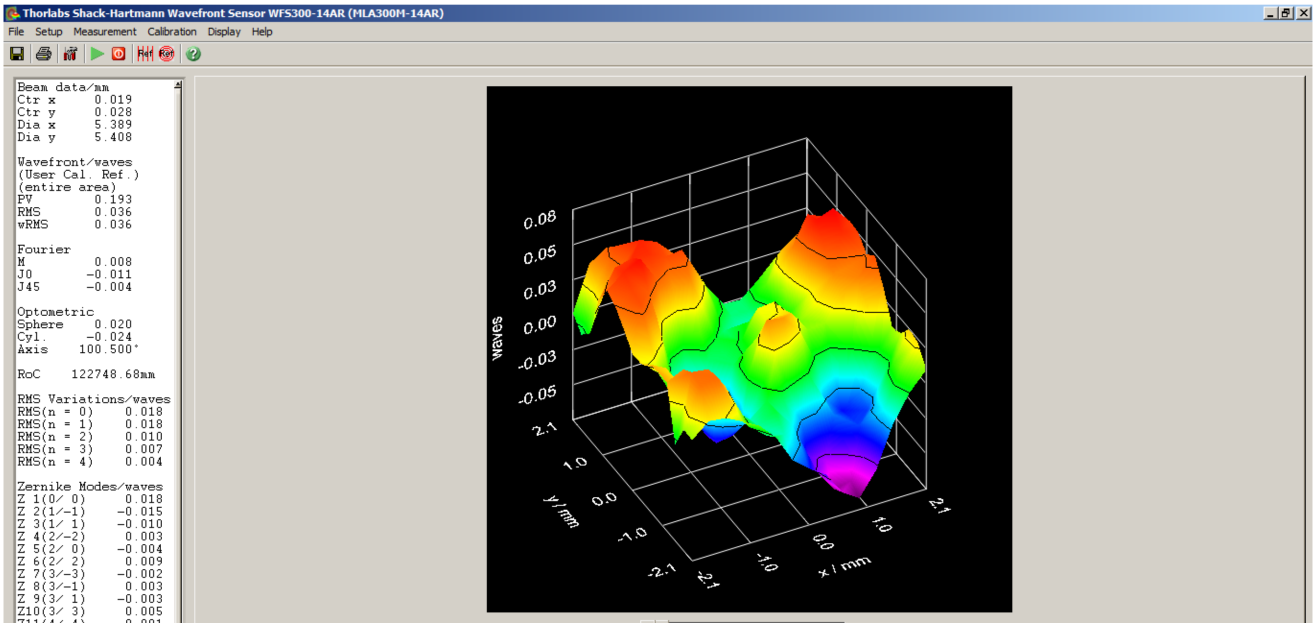

Figure 20: Return Wavefront after Double Pass

2.10.2.4 Double Pass Zernike Coefficients

The Zernike coefficients of the returned beam after two passes through the telescope are shown in Figure 21. The astigmatic coefficients, Z4 = 0.003, and Z6 = 0.009 are less than the requirement 0.02.

The largest coefficient, Z1 = 0.01 waves of piston, which is a constant phase offset and does not affect the wavefront. Z2 and Z3 are tilt coefficients, which were removed in software. Z5 = 0.004 waves is the defocus coefficient.

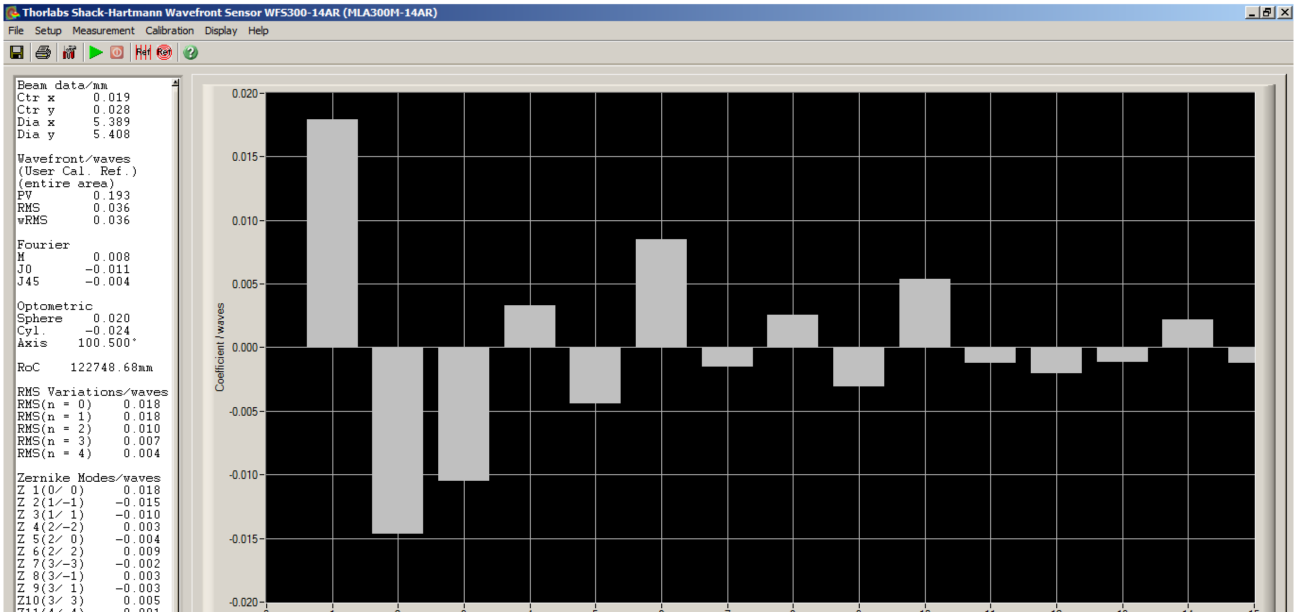

Figure 21: Double Pass Zernike Coefficients

The view through AC3 is shown in Figure 22. The focused reticle pattern is visible, together with the S. H. laser beam. Both patterns are centered with the cross hairs of AC3.

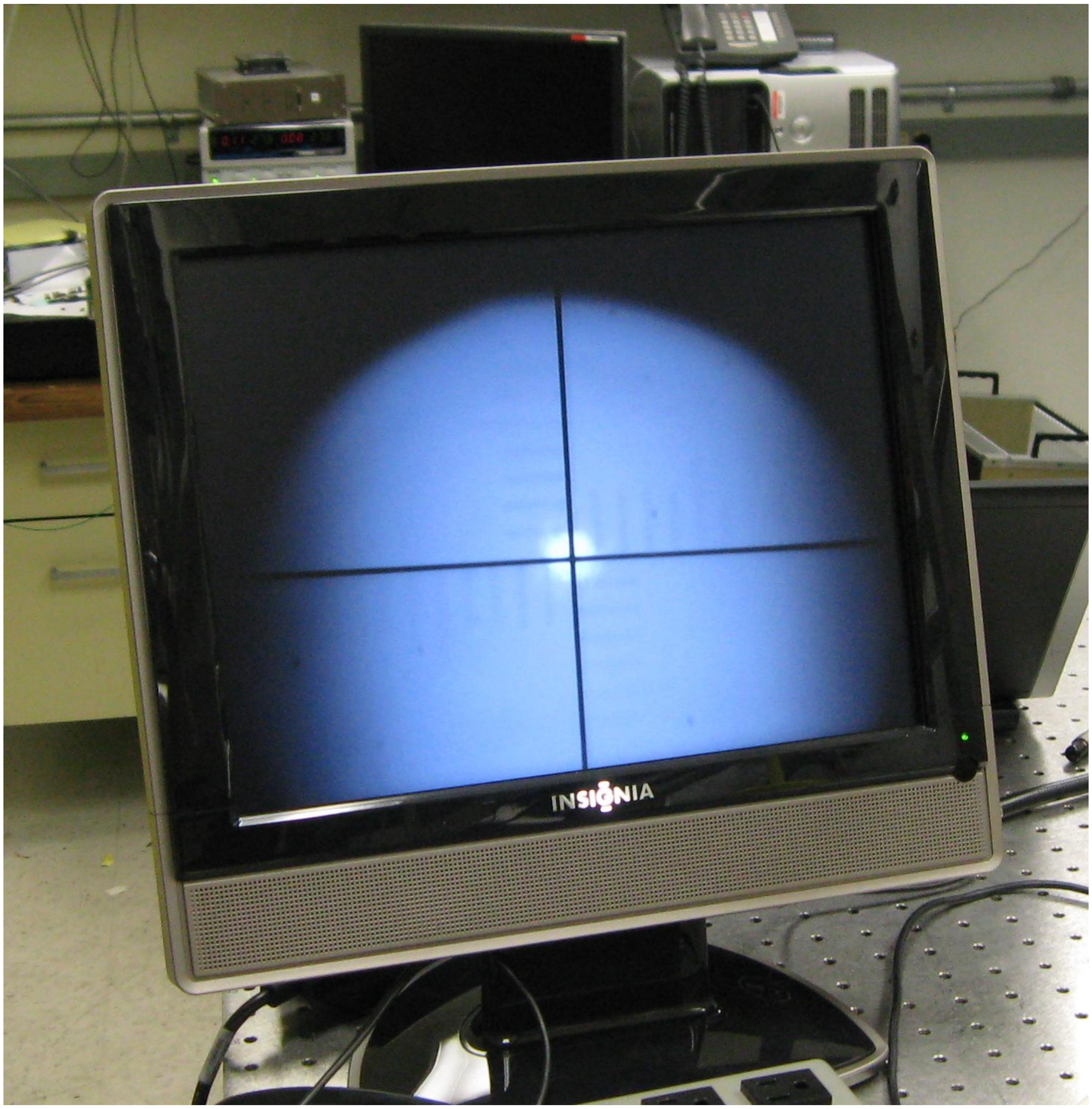

.

Figure 22: Double Pass Reticle Pattern with Centered Shack-Hartmann Laser Beam

3 Zemax Simulation

3.1 Initial Autocollimator Alignment

The autocollimator alignment procedure does not allow the 2ndary mirror to be tipped in pitch and yaw, only lateral translation and axial focusing.

After the initial autocollimator alignment, some astigmatism is still evident as seen in the spot diagram of Figure 23. The astigmatism results in a separation of the two astigmatic foci, as seen in Figure 24 and Figure 25, which cause a Guoy phase error at the focus of the TMS Guoy phase telescopes (a 100mm focal length lens was assumed for this simulation).

The Z5 and Z6 Zernike coefficients, as well as the saddle shaped wavefront indicate that astigmatism is present.

The output beam waist at the 2ndary mirror indicates wavefront curvature as shown in

Figure 28.

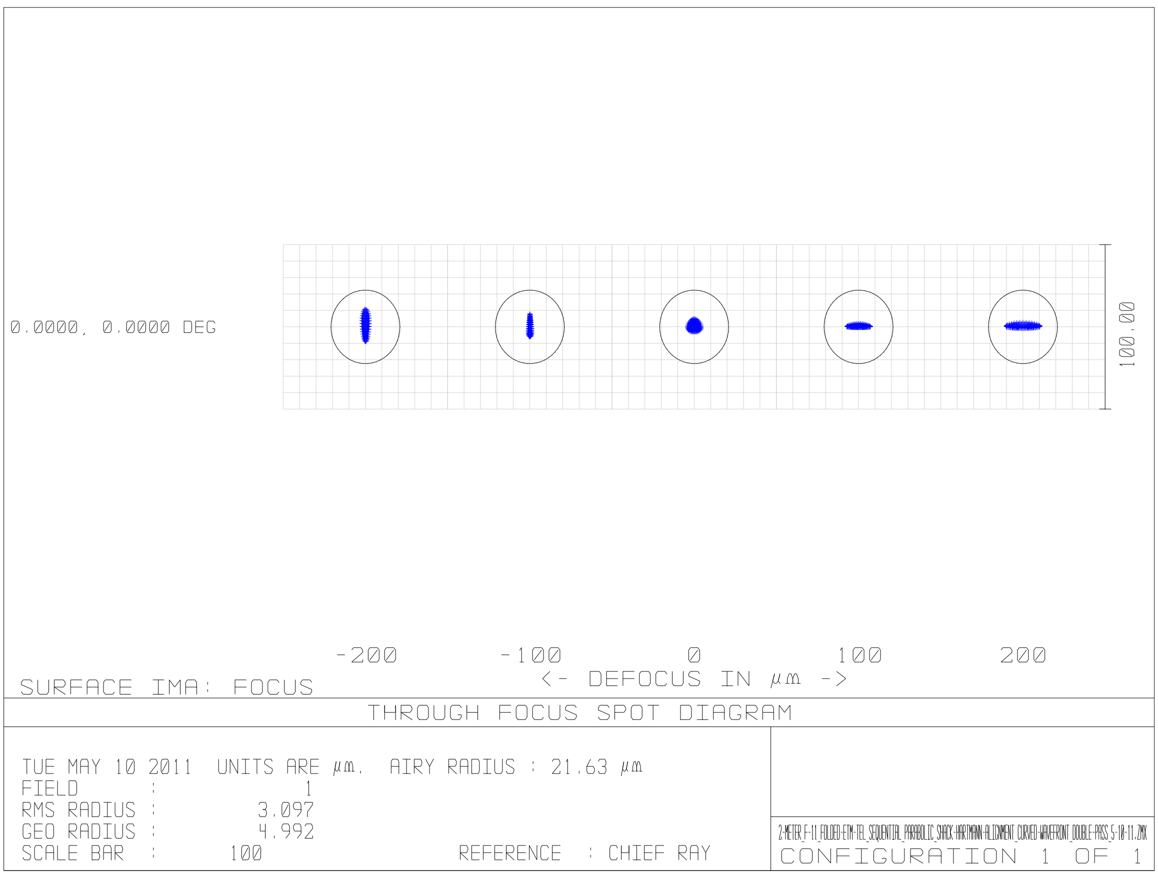

Figure 23: Spot Diagram Showing the Two Astigmatic Foci after Initial Autocollimator Alignment

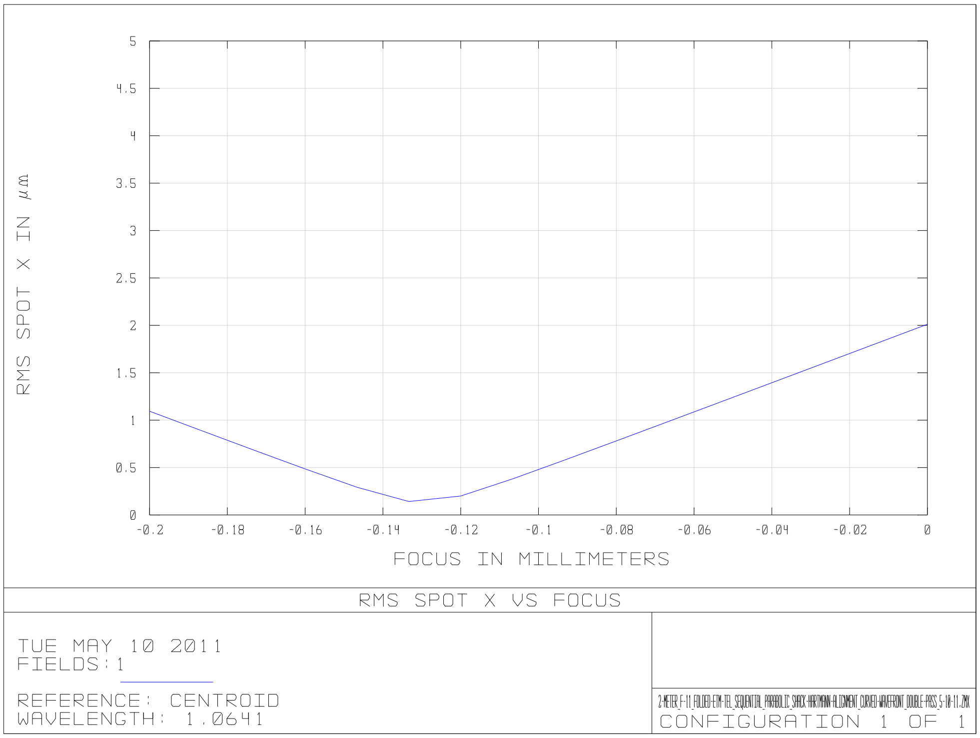

Figure 24: Left Shifted Focal Position of X-focus, after Initial Autocollimator Alignment

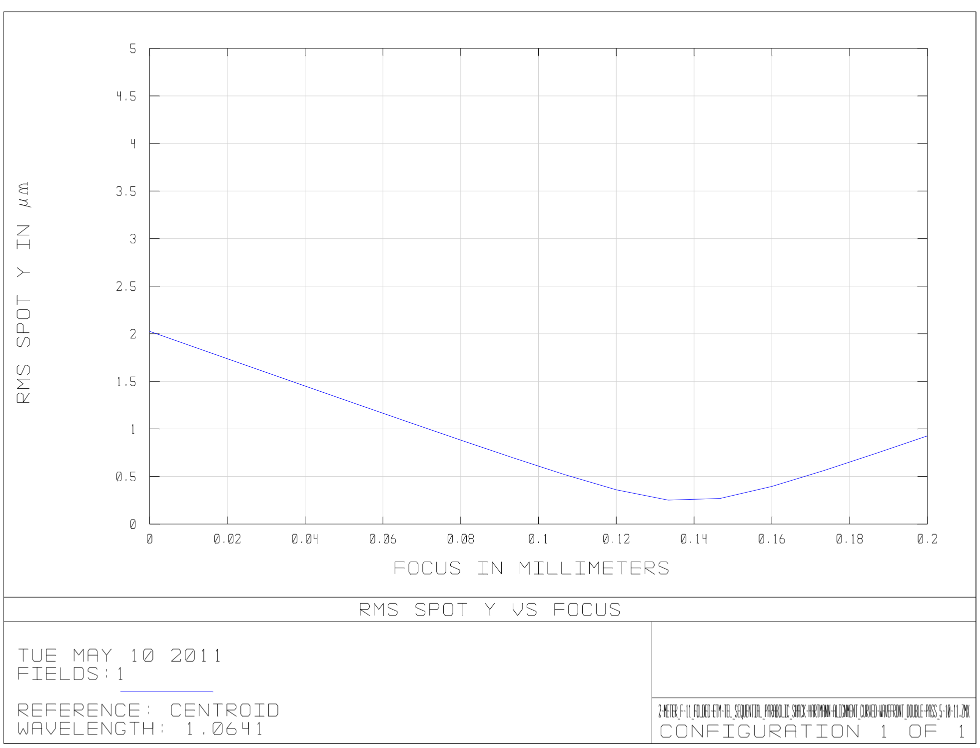

Figure 25: Right Shifted Focal Position of Y-focus, after Initial Autocollimator Alignment

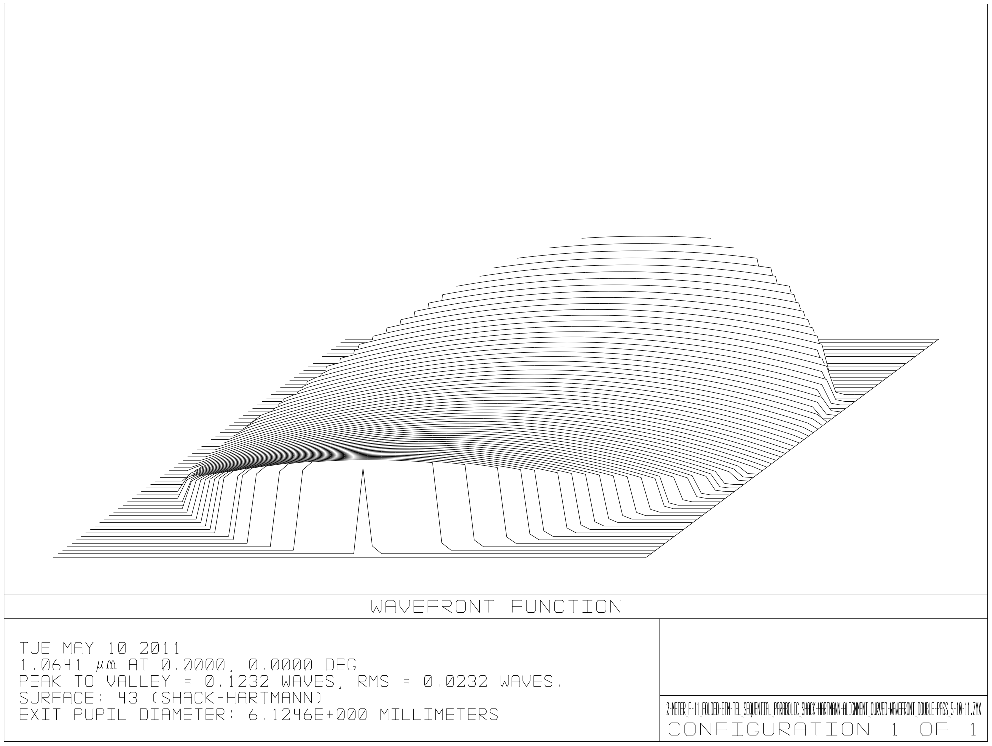

Figure 26: Wavefront of Double Pass Output Beam at 2ndary Mirror, after Initial Autocollimator Alignment

Listing of Zernike Standard Coefficient Data

Using Zernike Standard polynomials.

OPD referenced to chief ray.

Z 1 0.00086500 : 1

Z 2 0.00000003 : 4^(1/2) (p) * COS (A)

Z 3 0.00325350 : 4^(1/2) (p) * SIN (A)

Z 4 0.00045882 : 3^(1/2) (2p^2 - 1)

Z 5 -0.00000038 : 6^(1/2) (p^2) * SIN (2A)

Z 6 -0.02314406 : 6^(1/2) (p^2) * COS (2A)

Z 7 0.00114957 : 8^(1/2) (3p^3 - 2p) * SIN (A)

Z 8 0.00000001 : 8^(1/2) (3p^3 - 2p) * COS (A)

Z 9 -0.00006707 : 8^(1/2) (p^3) * SIN (3A)

Z 10 0.00000000 : 8^(1/2) (p^3) * COS (3A)

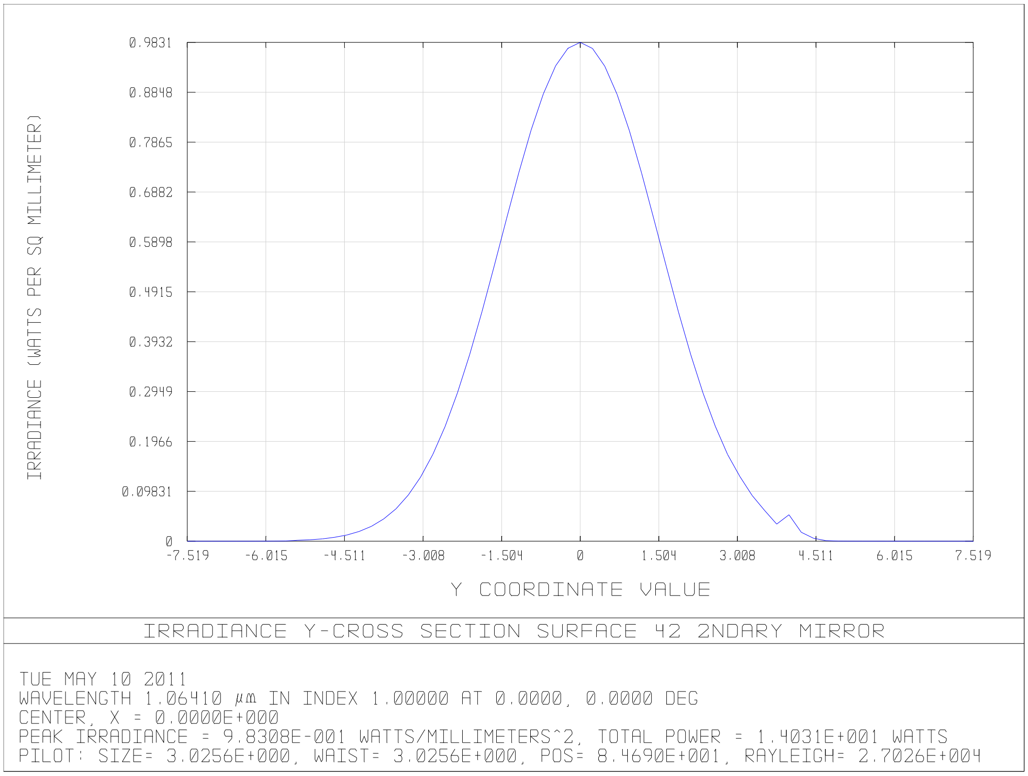

Figure 27: Output Beam Profile at 2ndary Mirror. after Initial Autocollimator Alignment

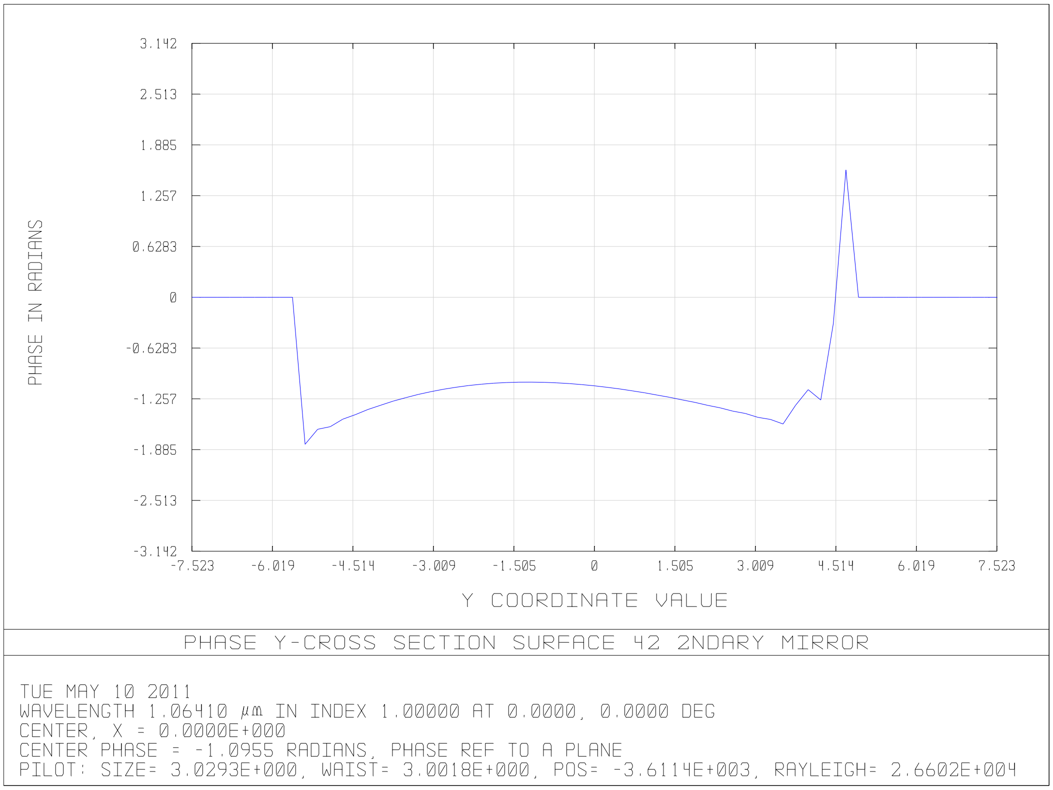

Figure 28: Output Beam Phase at 2ndary Mirror, after Initial Autocollimator Alignment

3.2 ZEMAX Interferometer Arm Cavity Beam Propagation Through Transmon System

The IFO arm cavity beam was modeled as a Gaussian beam with a 12.01mm beam waist (radius) located 2161m in front of the ETM HR mirror. The beam arrives at the ETM HR with a curvature of 2245m, concave toward the IFO beam waist, and is collimated to a beam waist at the 2ndary mirror of the telescope. The transmon beam exiting the telescope is focused by a 100 mm ideal lens to simulate the TMS Guoy lens . The wavefront properties of the focused beam are described in terms of Zernike coefficients. The telescope is aligned to minimize the Zernike astigmatic coefficients.

The ZEMAX single pass optical layout is shown in Figure 29.

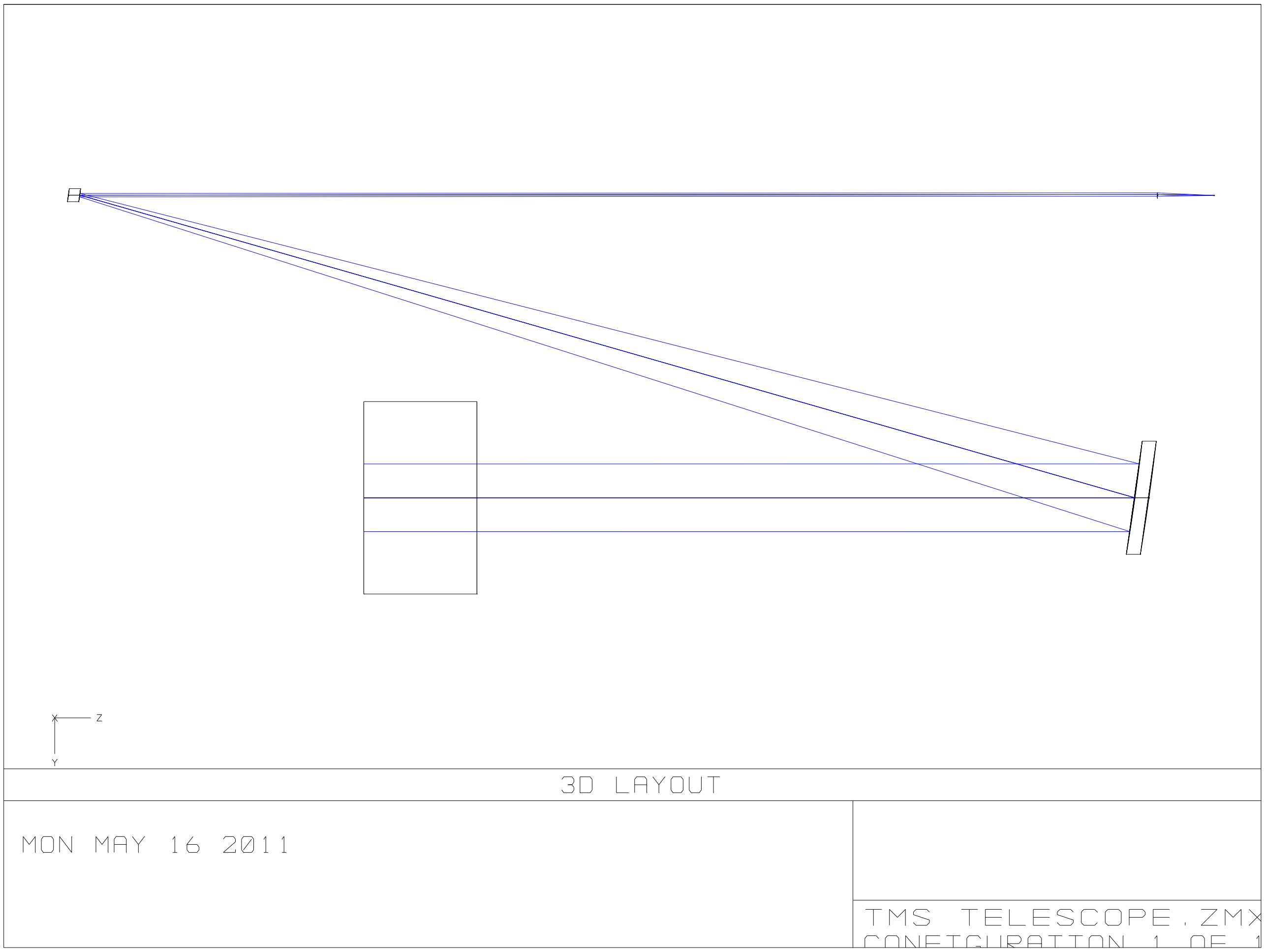

Figure 29: IFO Beam Propagation Model from IFO Beam Waist through the Transmon Optical System.

3.3 ZEMAX Double Pass Alignment of TMS Telescope Using Shack-Hartmann Sensor

The TMS telescope was aligned using ZEMAX by launching a Gaussian beam with a 3.103 mm radius waist at the 2ndary mirror, passing the beam through the telescope, and retro-reflecting the beam from a mirror placed at the entrance of the telescope to make a double pass through the telescope back to the 2ndary mirror. The ZEMAX program optimized the telescope alignment by minimizing the Zernike astigmatism coefficients and by setting the output beam curvature either to zero, or to a specified value at the 2ndary mirror.

Two choices of retro-reflecting mirror will be considered in the following ZEMAX models--1) ETM HR surrogate, and 2) flat mirror.

3.3.1 ETM HR Surrogate

A double pass sequential beam ray trace is shown in Figure 30. The ETM mirror has been included in the model to correctly model the IFO beam propagation.

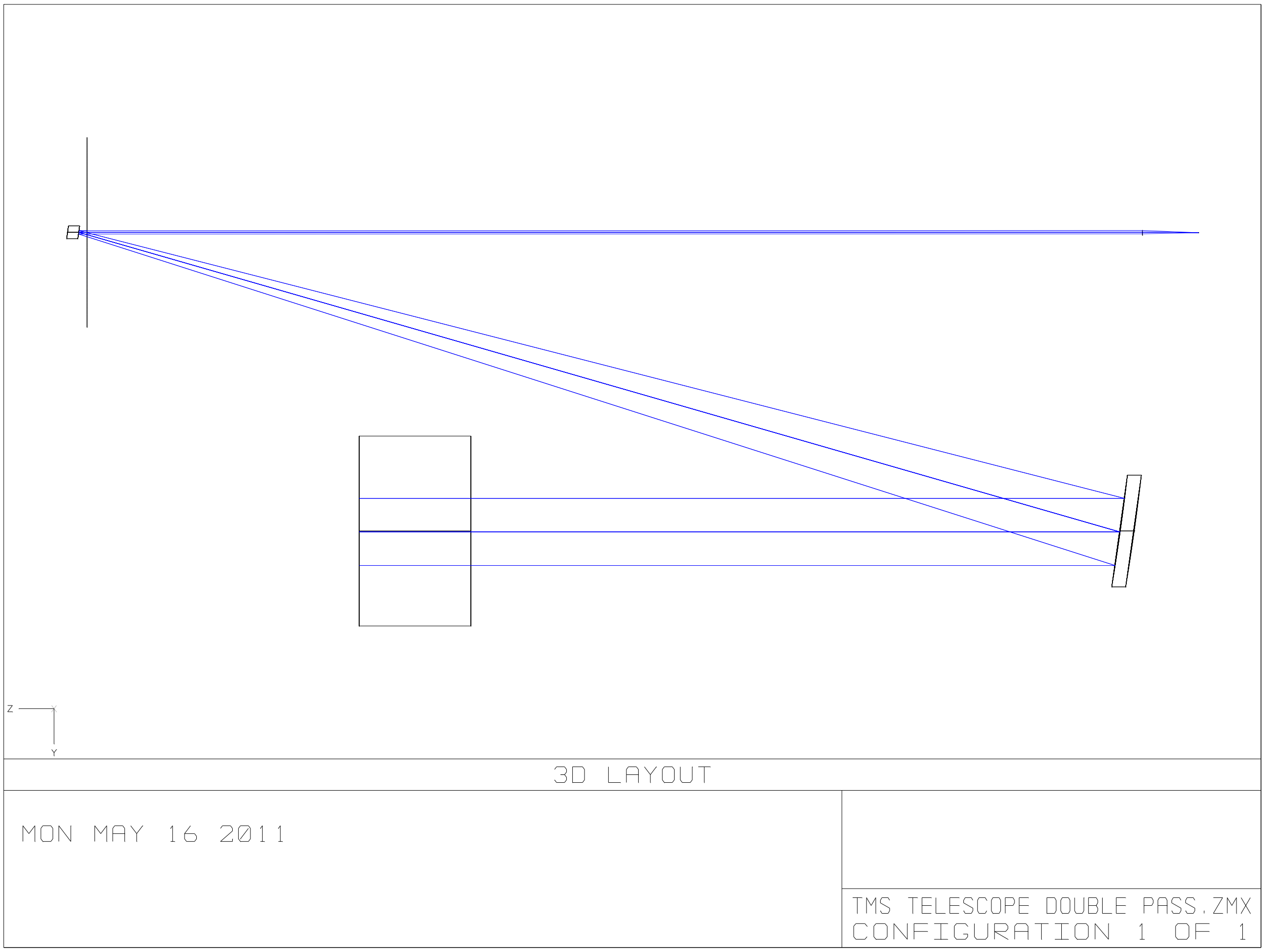

Figure 30: ZEMAX Sequential Ray Trace of Double Pass through Telescope with ETM Surrogate Mirror

The ZEMAX physical optics propagation program is also used to analyze the beam propagation. A 3.103 mm radius beam with a flat beam waist is injected at the 2ndary mirror, as shown in Figure 31 and Figure 32.

The output beam parameters at the 2ndary mirror after the double pass are shown in Figure 33 and Figure 34. The output beam diameter is approximately 3 mm radius, and the wavefront is relatively flat across the central portion of the beam.

The output beam parameters are also shown at the location of the Shack-Hartmann sensor, as shown in **Error! Reference source not found.** and Figure 35.

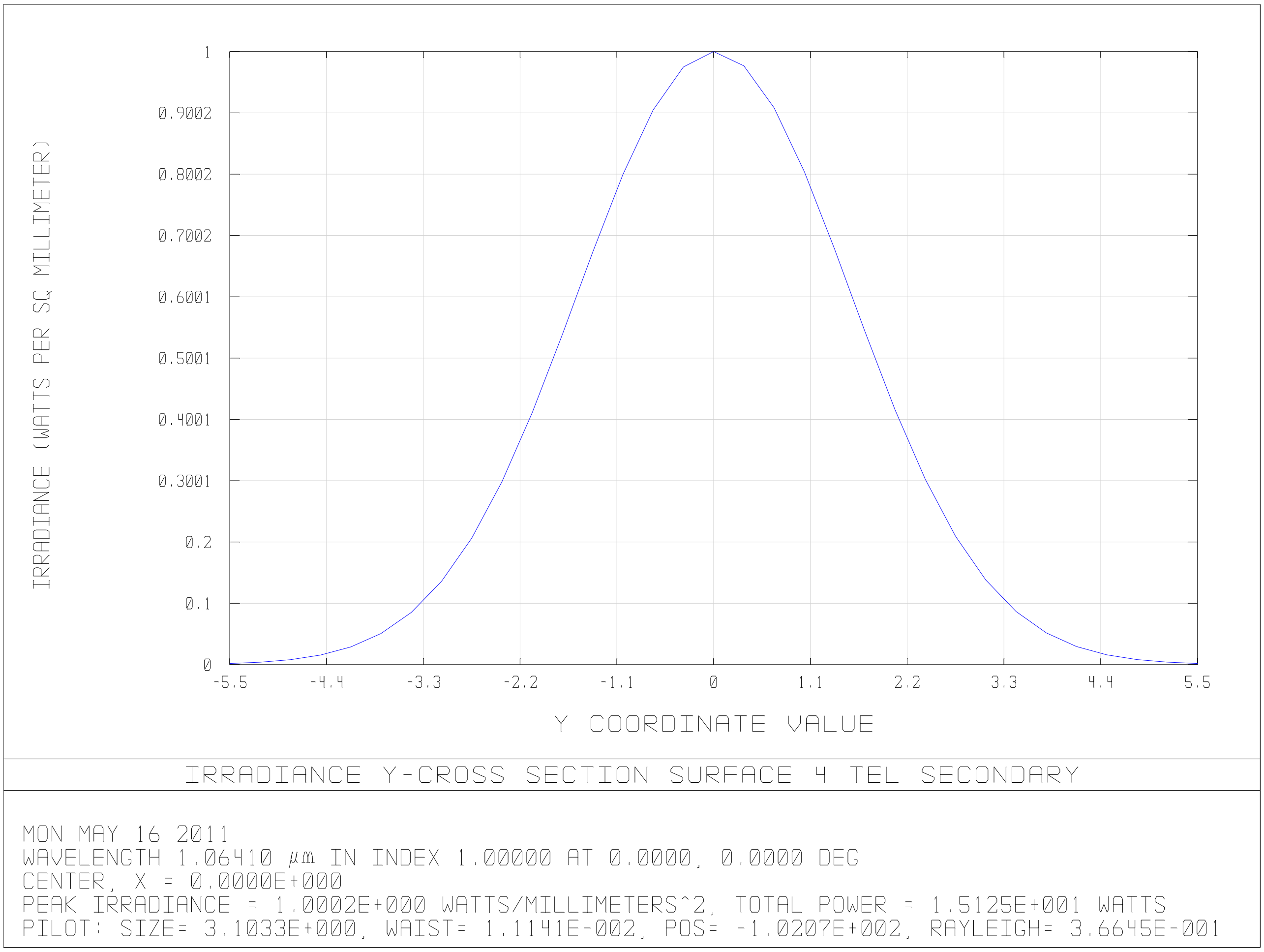

Figure 31: Input Beam Waist Cross Section at 2ndary Mirror, with ETM Surrogate Mirror

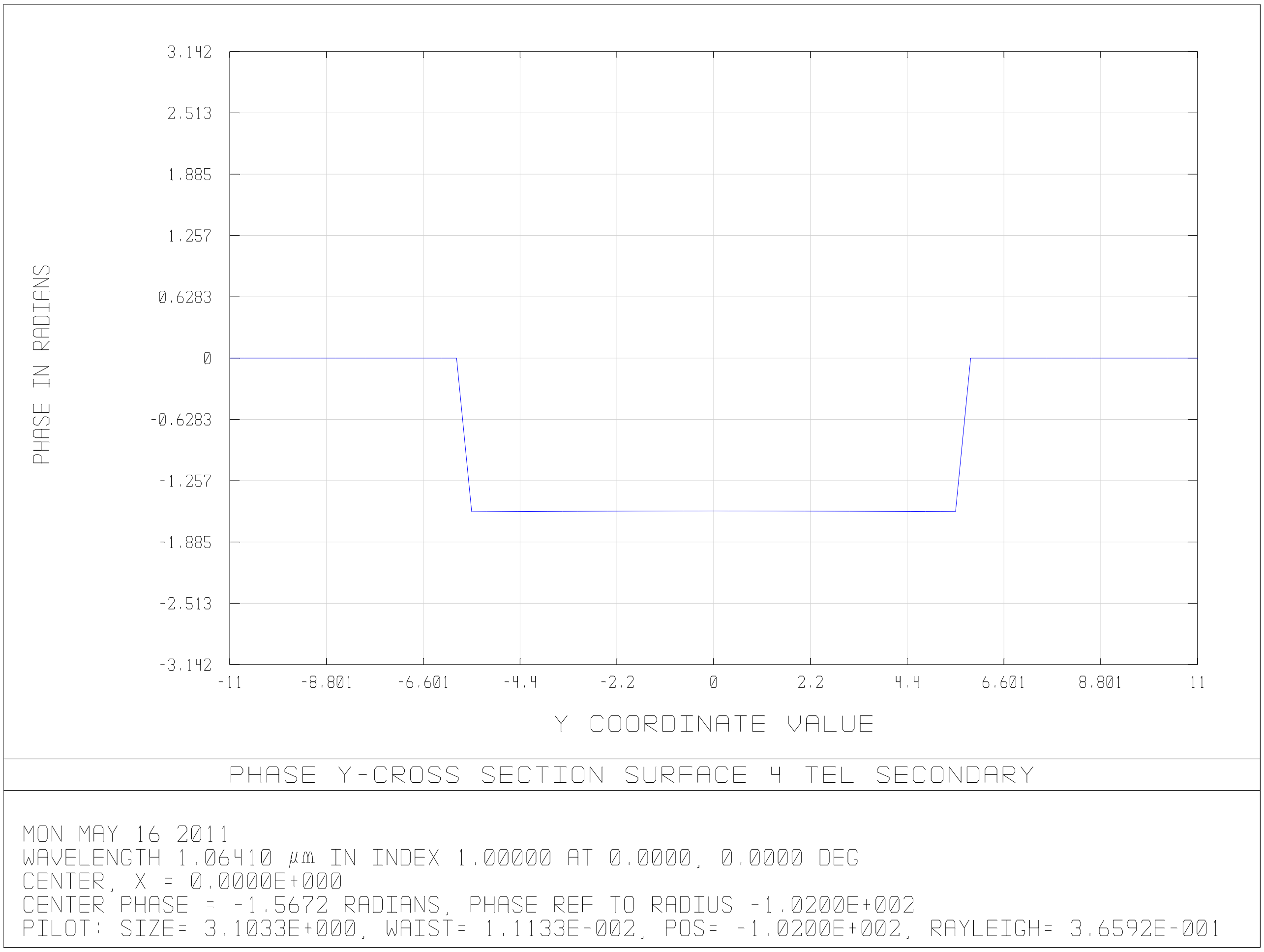

Figure 32: Phase of Input Beam Waist at 2ndary Mirror, with ETM Surrogate Mirror

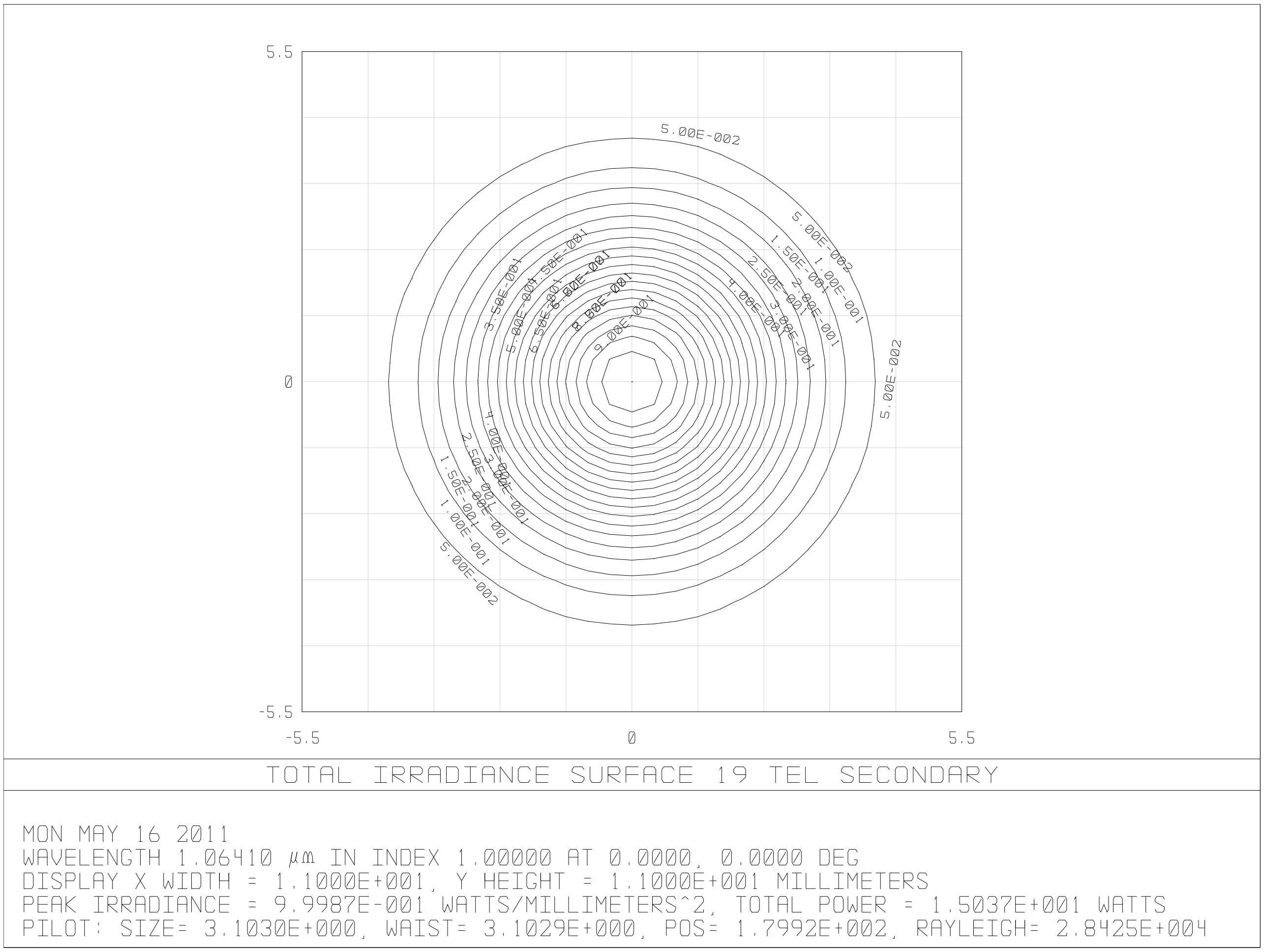

Figure 33: Cross Section of Output Beam at 2ndary Mirror, with ETM Surrogate Mirror

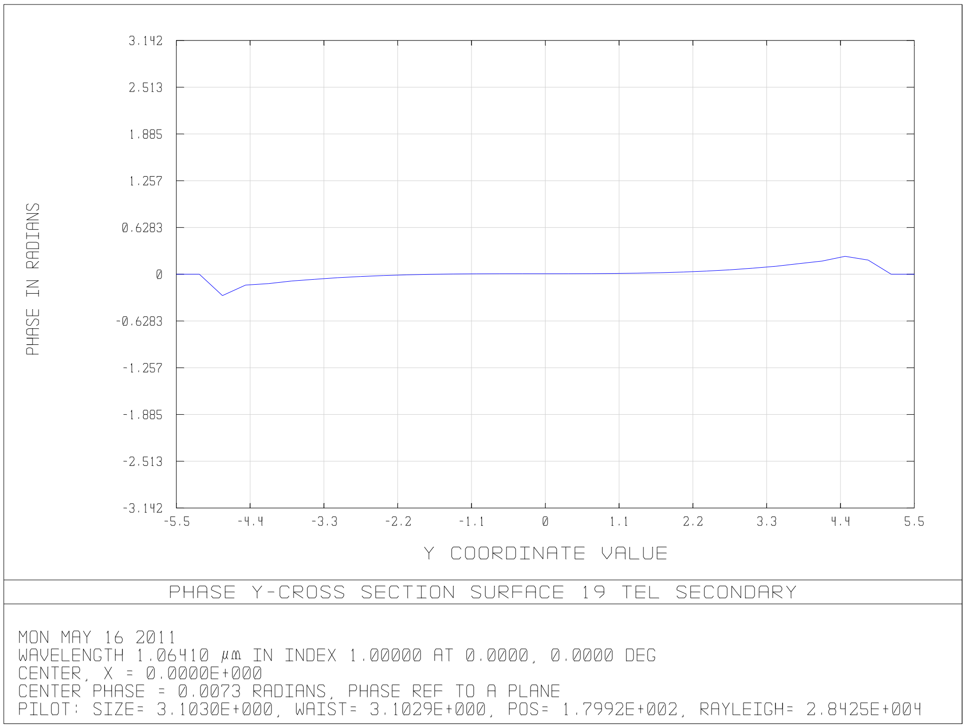

Figure 34: Phase of Output Beam at 2ndary Mirror, with ETM Surrogate Mirror

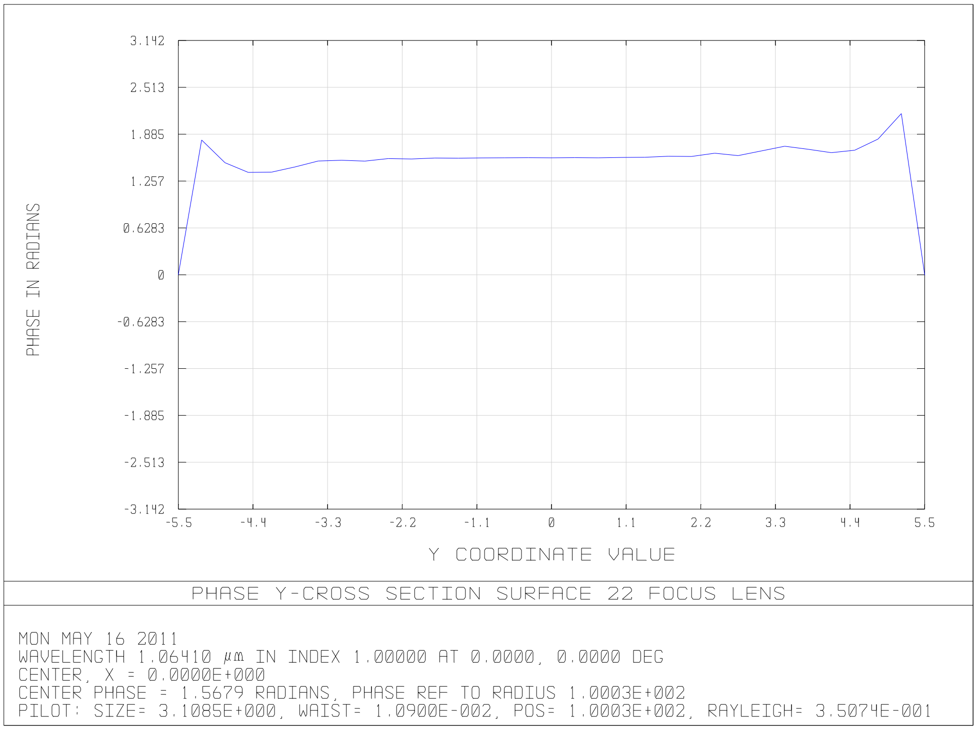

Figure 35: Phase of Output Beam at Shack-Hartmann Sensor Location, with ETM Surrogate Mirror

The phase map of the output beam is shown in Figure 36.

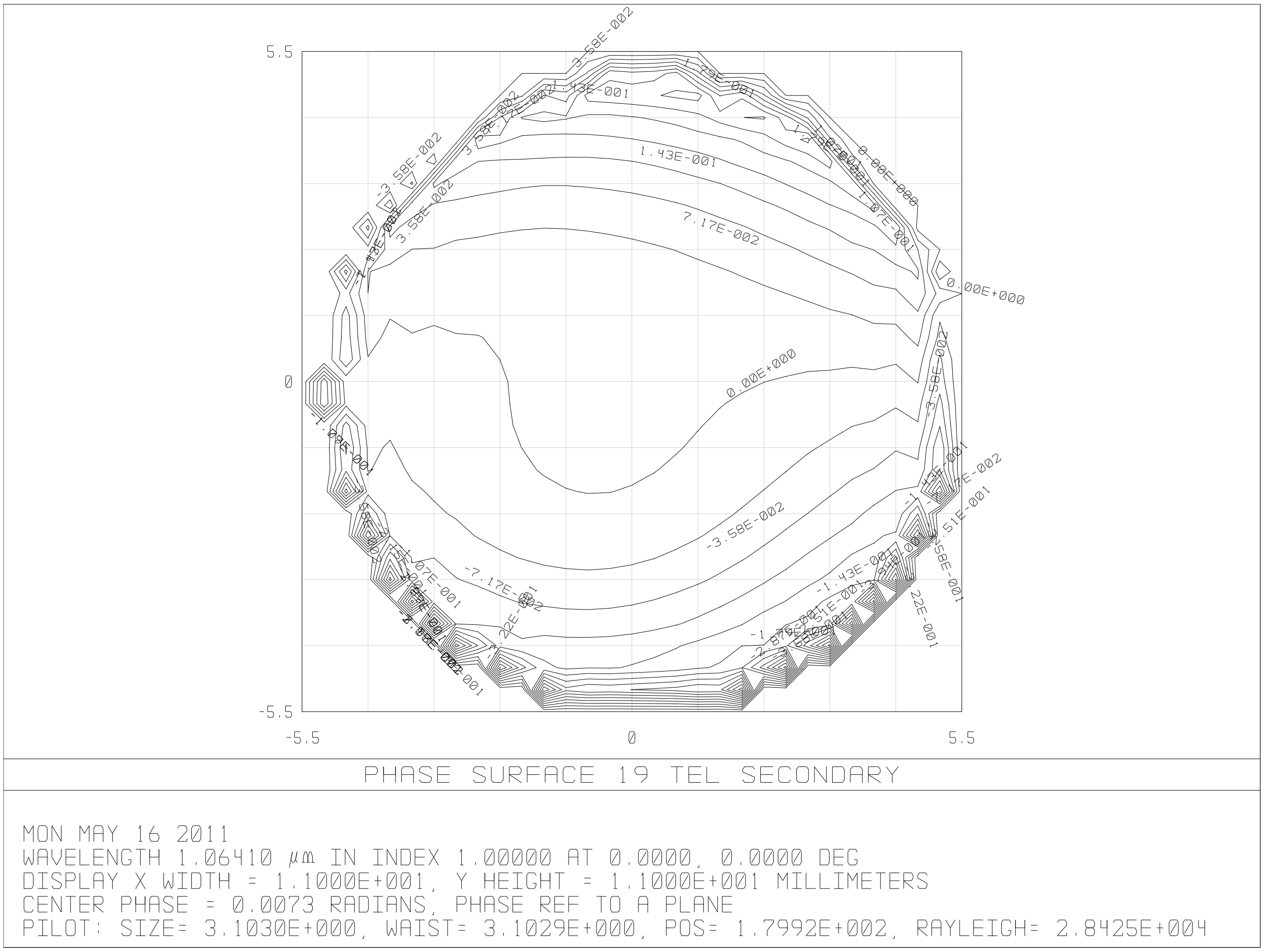

Figure 36: Phase Map of Output Beam, with ETM Surrogate Mirror

Listing of Zernike Standard Coefficient Data

Surface : Image

Field : 0.0000, 0.0000 deg

Wavelength : 1.0641 µm

From integration of the fitted coefficients:

RMS (to chief) : 0.01010235 waves

RMS (to centroid) : 0.00997530 waves

Variance : 0.00009951 waves squared

Strehl Ratio (Est) : 0.99607934

RMS fit error : 0.00001552 waves

Maximum fit error : 0.00003968 waves

Z 1 -0.01707594 : 1

Z 2 -0.00003487 : 4^(1/2) (p) * COS (A)

Z 3 -0.00159677 : 4^(1/2) (p) * SIN (A)

Z 4 -0.00987879 : 3^(1/2) (2p^2 - 1)

Z 5 -0.00038791 : 6^(1/2) (p^2) * SIN (2A)

Z 6 0.00120293 : 6^(1/2) (p^2) * COS (2A)

Z 7 -0.00056424 : 8^(1/2) (3p^3 - 2p) * SIN (A)

Z 8 -0.00001233 : 8^(1/2) (3p^3 - 2p) * COS (A)

Z 9 -0.00000150 : 8^(1/2) (p^3) * SIN (3A)

Z 10 -0.00000041 : 8^(1/2) (p^3) * COS (3A)

Z4 is the curvature, and Z5 and Z6 are the astigmatic coefficients. The coefficients meet the minimum requirements.

3.3.2 Astigmatic Foci Displacement after Simulated Shack-Hartmann Alignment

As a result of the simulated Shack-Hartmann alignment, the astigmatism is reduced, and the astigmatic focal planes coincide, as shown in Figure 37, Figure 38, and Figure 39.

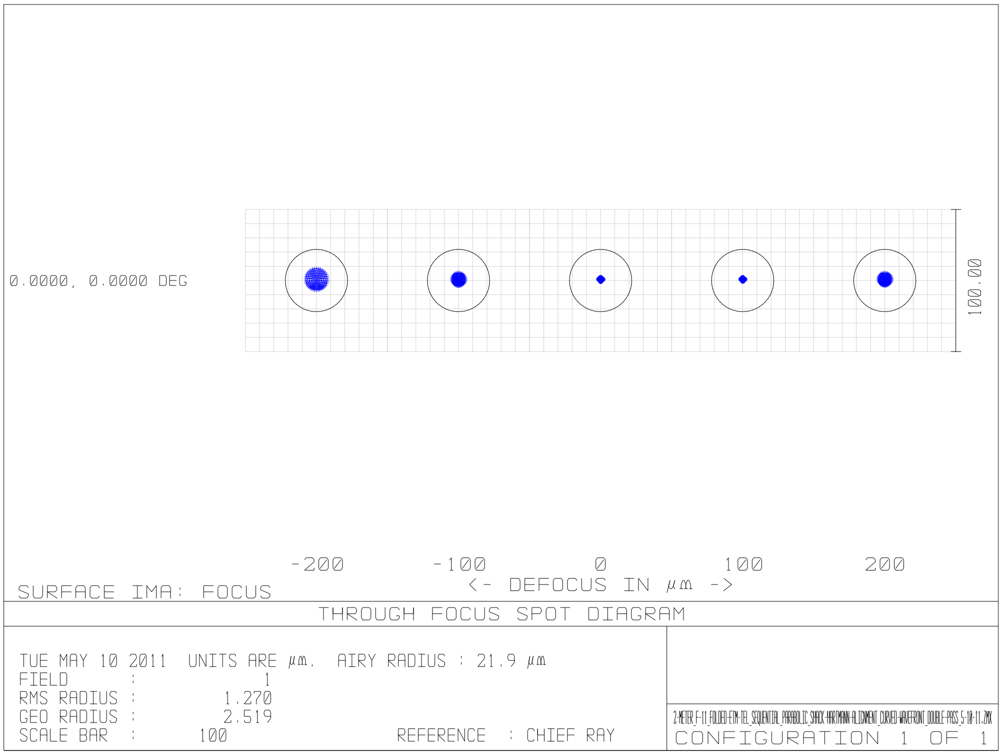

Figure 37: Spot Diagram Showing No Astigmatic Foci

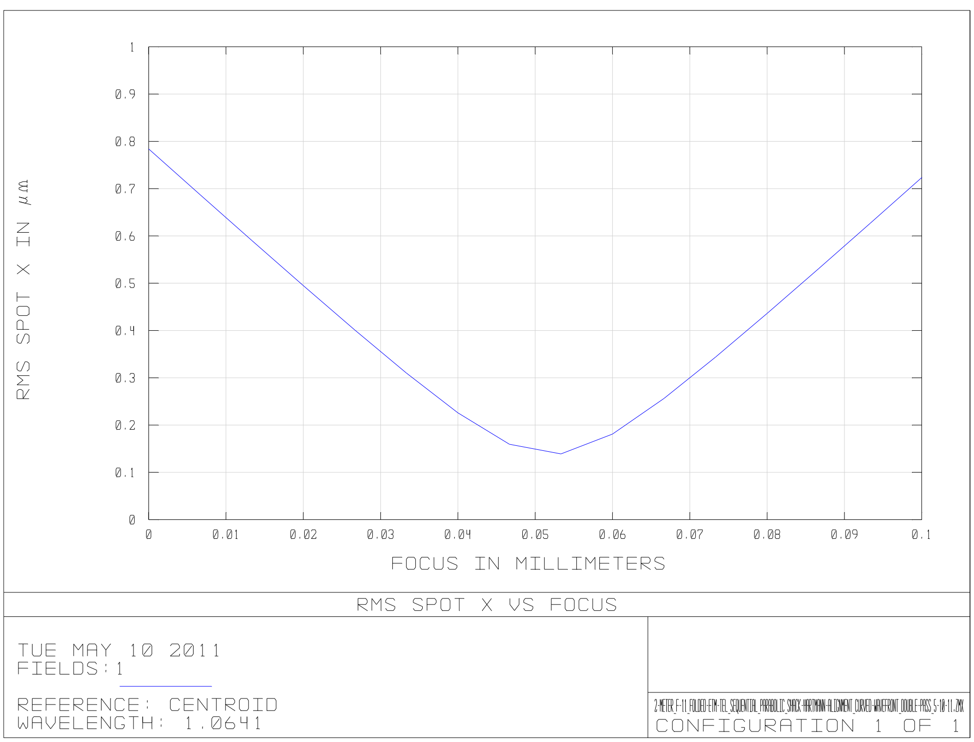

Figure 38: No Shift of X-focus

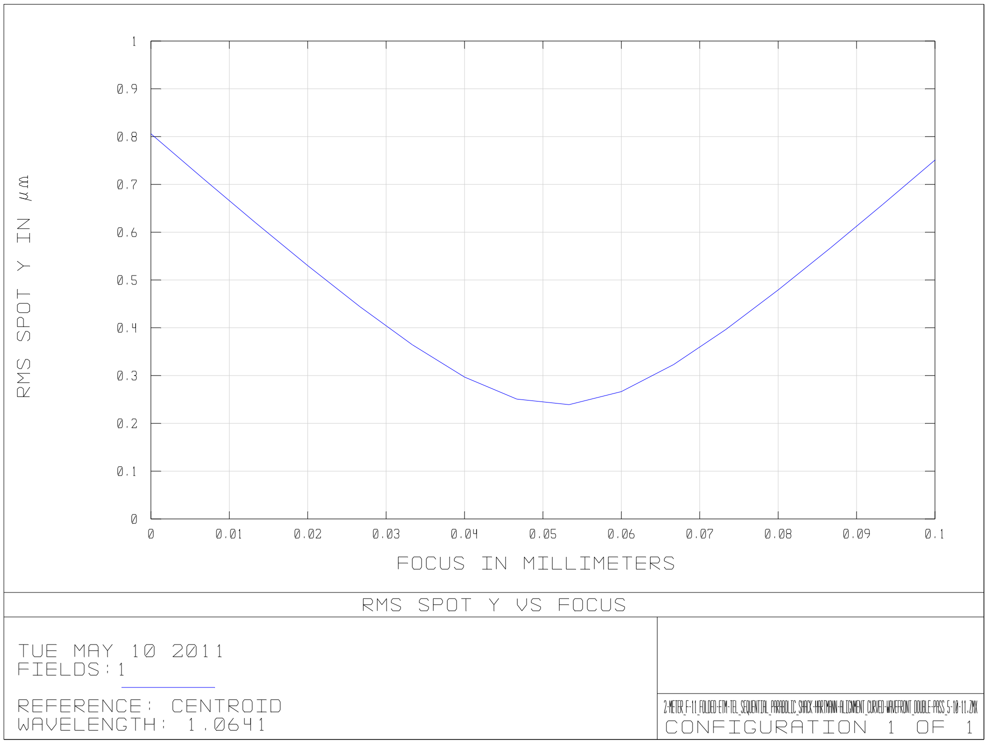

Figure 39: No Shift of Y-focus

3.3.2.1 Check of the IFO Beam Propagation with the ETM HR Surrogate Alignment

The telescope alignment parameters from the double pass alignment were inserted the IFO Beam Propagation Model, and the results are shown below.

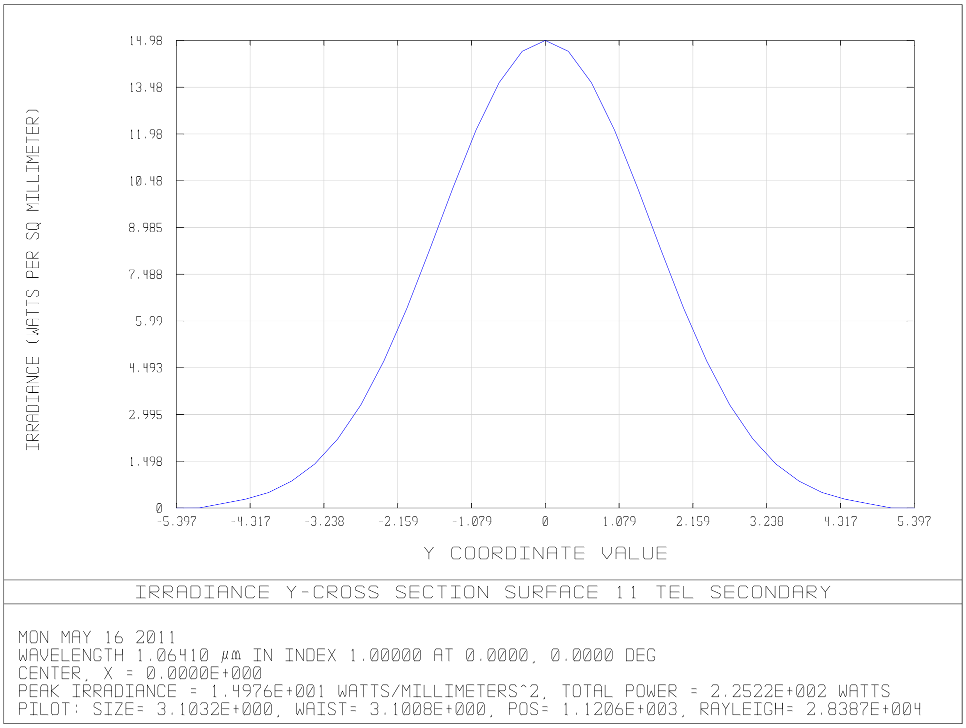

Figure 40: Cross Section of IFO Output Beam at 2ndary Mirror of Aligned Telescope, with ETM HR Surrogate

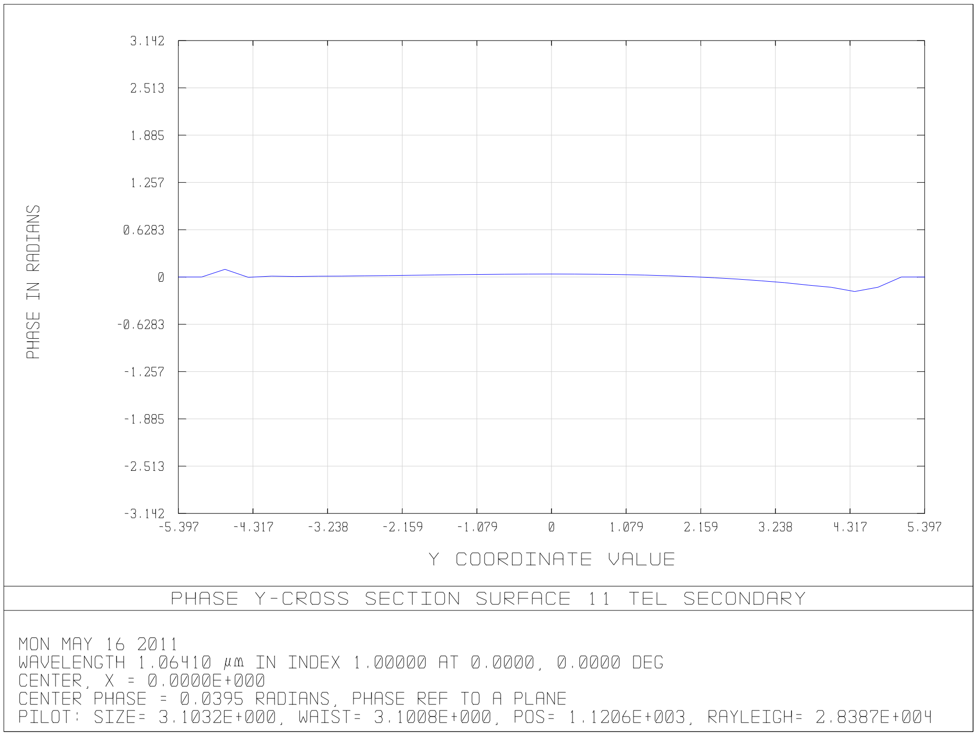

Figure 41: Phase of IFO Output Beam at 2ndary Mirror of Aligned Telescope, with ETM HR Surrogate

Listing of Zernike Standard Coefficient Data

Surface : Image

Field : 0.0000, 0.0000 deg

Wavelength : 1.0641 µm

From integration of the fitted coefficients:

RMS (to chief) : 0.01010235 waves

RMS (to centroid) : 0.00997530 waves

Variance : 0.00009951 waves squared

Strehl Ratio (Est) : 0.99607934

RMS fit error : 0.00001552 waves

Maximum fit error : 0.00003968 waves

Z 1 -0.01707594 : 1

Z 2 -0.00003487 : 4^(1/2) (p) * COS (A)

Z 3 -0.00159677 : 4^(1/2) (p) * SIN (A)

Z 4 -0.00987879 : 3^(1/2) (2p^2 - 1)

Z 5 -0.00038791 : 6^(1/2) (p^2) * SIN (2A)

Z 6 0.00120293 : 6^(1/2) (p^2) * COS (2A)

Z 7 -0.00056424 : 8^(1/2) (3p^3 - 2p) * SIN (A)

Z 8 -0.00001233 : 8^(1/2) (3p^3 - 2p) * COS (A)

Z 9 -0.00000150 : 8^(1/2) (p^3) * SIN (3A)

Z 10 -0.00000041 : 8^(1/2) (p^3) * COS (3A)

The Zernike Z5 and Z6 coefficients are <0.02, indicating that the Guoy phase error at the focus of the 100 mm lens is < 10 deg.

3.3.3 Alternate Flat Mirror Alignment

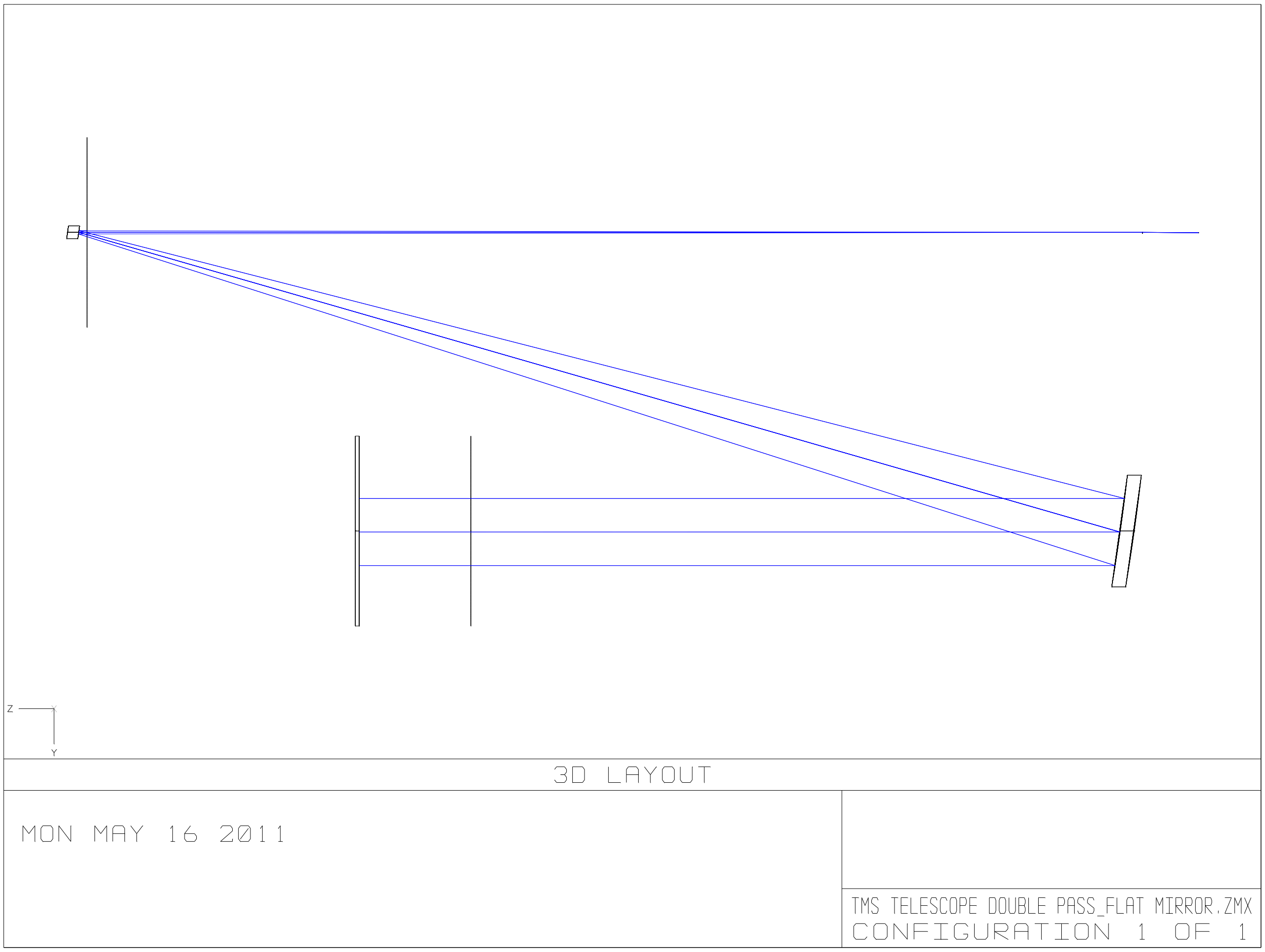

Figure 42: Optical Layout for Double Pass Flat Mirror Alignment

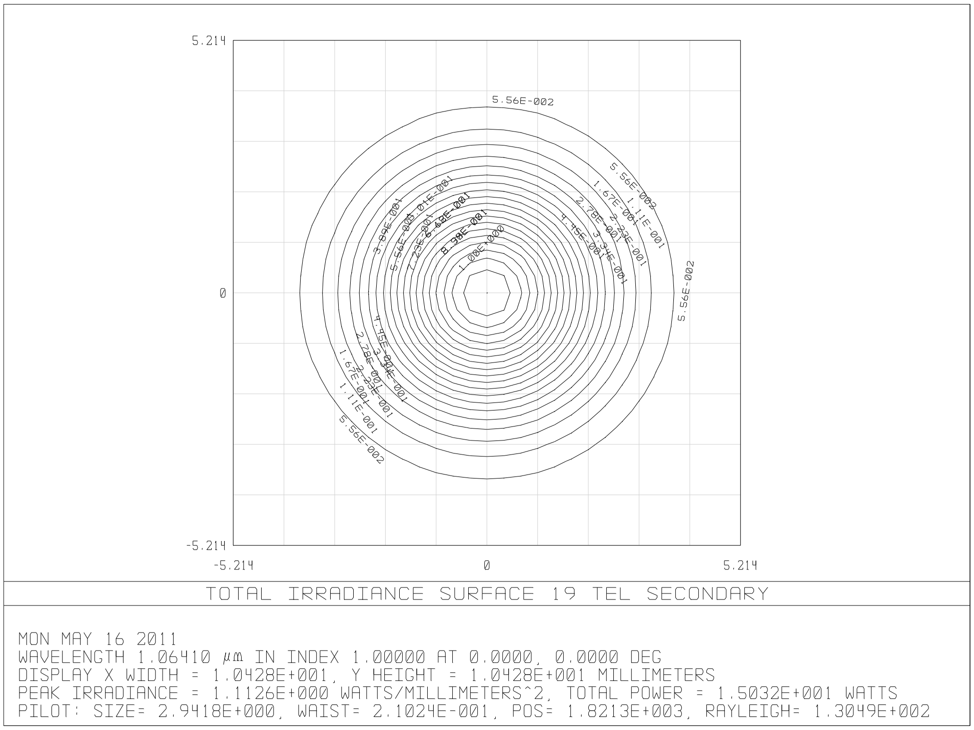

Figure 43: Cross Section of Output Beam at 2ndary Mirror, with Flat Mirror

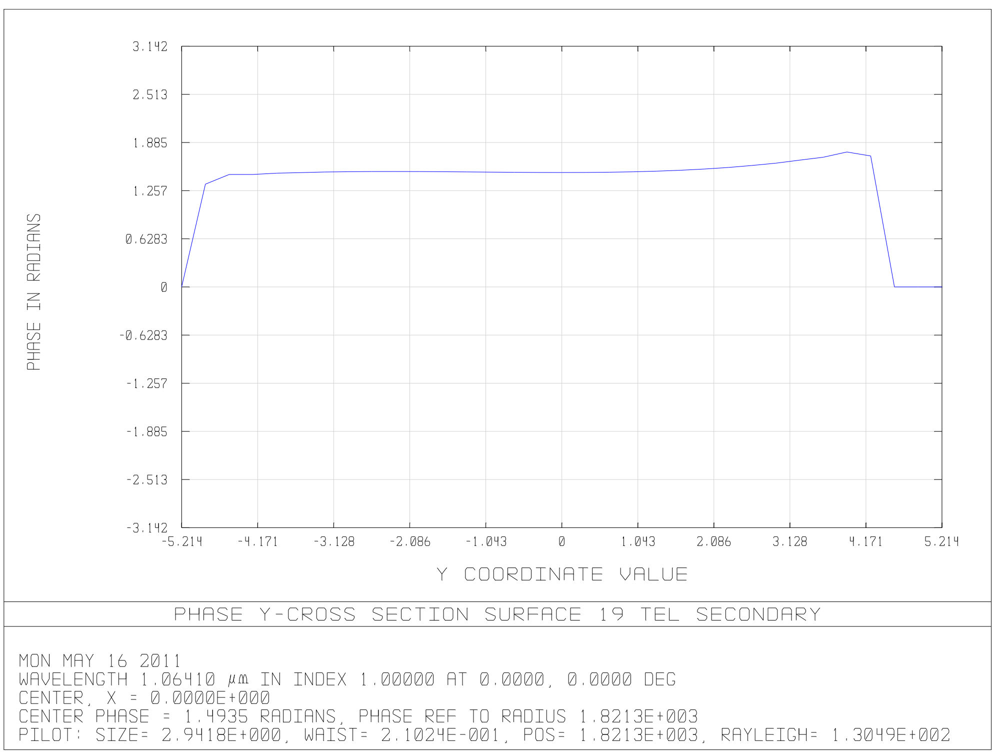

Figure 44: Phase of Output Beam at 2ndary Mirror, with Flat Mirror

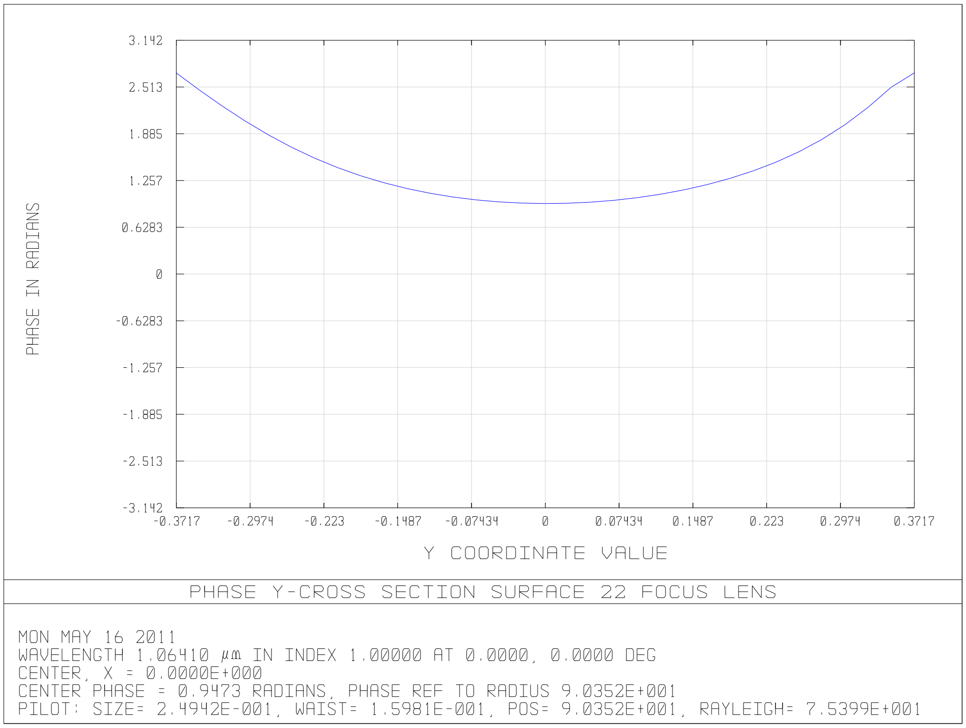

Figure 45: Phase of Output Beam at Shack-Hartmann Sensor Location, with Flat Mirror

Listing of Zernike Standard Coefficient Data

Using Zernike Standard polynomials.

OPD referenced to chief ray.

Surface : 22

Field : 0.0000, 0.0000 deg

Wavelength : 1.0641 µm

From integration of the fitted coefficients:

RMS (to chief) : 0.00387995 waves

RMS (to centroid) : 0.00285939 waves

Variance : 0.00000818 waves squared

Strehl Ratio (Est) : 0.99967727

RMS fit error : 0.00003324 waves

Maximum fit error : 0.00007825 waves

Z	1	0.00449645 :	1
Z	2	-0.00002849 :	4^(1/2) (p) * COS (A)
Z	3	-0.00262242 :	4^(1/2) (p) * SIN (A)
Z	4	0.00255312 :	3^(1/2) (2p^2 - 1)
Z	5	-0.00042542 :	6^(1/2) (p^2) * SIN (2A)
Z	6	-0.00078515 :	6^(1/2) (p^2) * COS (2A)
Z	7	-0.00092743 :	8^(1/2) (3p^3 - 2p) * SIN (A)
Z	8	-0.00001008 :	8^(1/2) (3p^3 - 2p) * COS (A)
Z	9	-0.00000106 :	8^(1/2) (p^3) * SIN (3A)
Z	10	0.00000044 :	8^(1/2) (p^3) * COS (3A)

Note that the focus Zernike coefficient, Z4 = 0.00255, was purposely adjusted by forcing the focus of the telescope to be the same as with the ETM HR surrogate mirror, to compensate for the telescope alignment with the flat mirror instead of the ETM HR surrogate mirror.

3.3.3.1 Check of the IFO Beam Propagation with the Flat Mirror Alignment

The telescope alignment parameters from the flat mirror double pass alignment were inserted the IFO Beam Propagation Model, and the results are shown below.

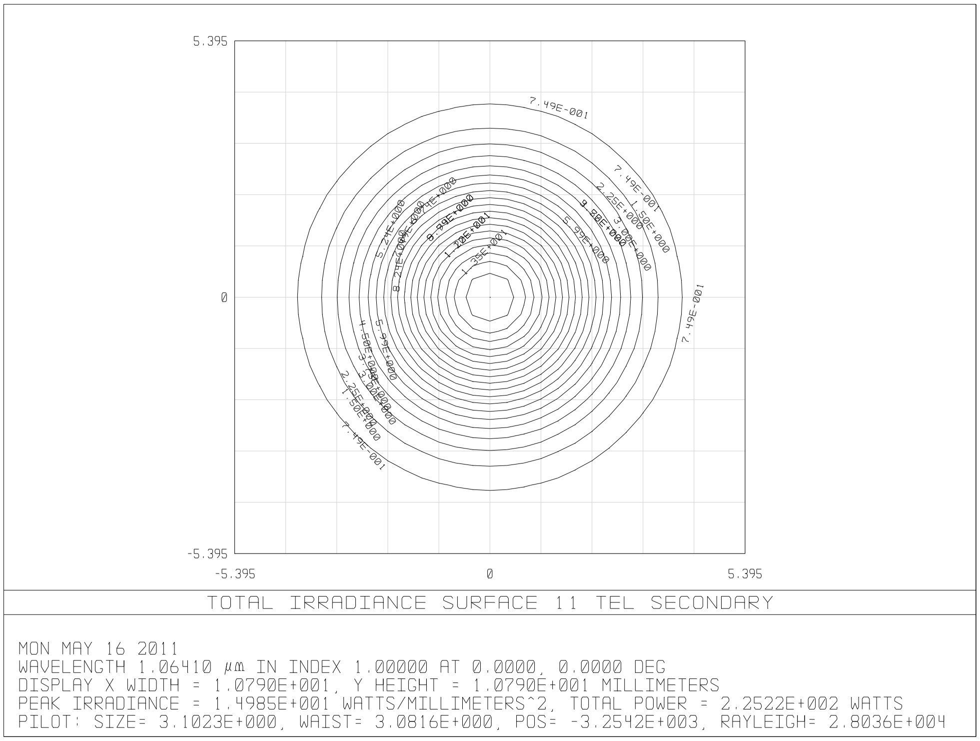

Figure 46: Contour of IFO Output Beam Cross Section at 2ndary Mirror, with Flat Mirror

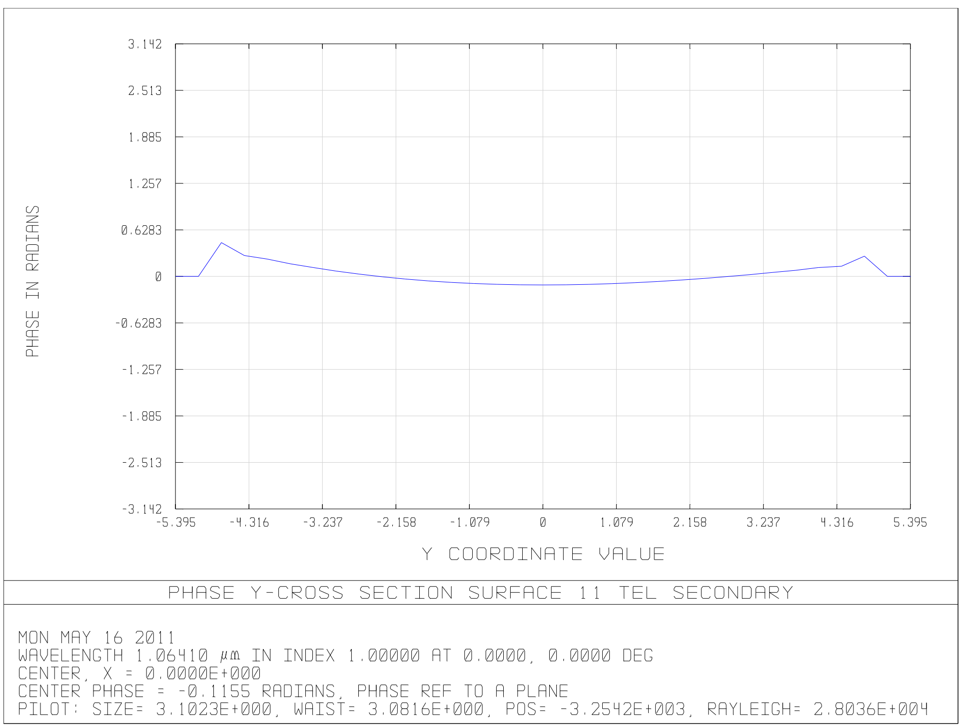

Figure 47: Phase of IFO Output Beam at 2ndary Mirror, with Flat Mirror

3.3.4 Telescope Performance with Non-Gaussian Input Beams

The Telescope was aligned using the Shack-Hartmann sensor to minimize the astigmatic aberrations and to minimize the curvature at the 2ndary mirror after a double pass.

A worst-case non-Gaussian, "top hat" beam profile with a flat wave front was launched into the secondary mirror; the beam profile and phase are shown in Figure 48 and Figure 49.

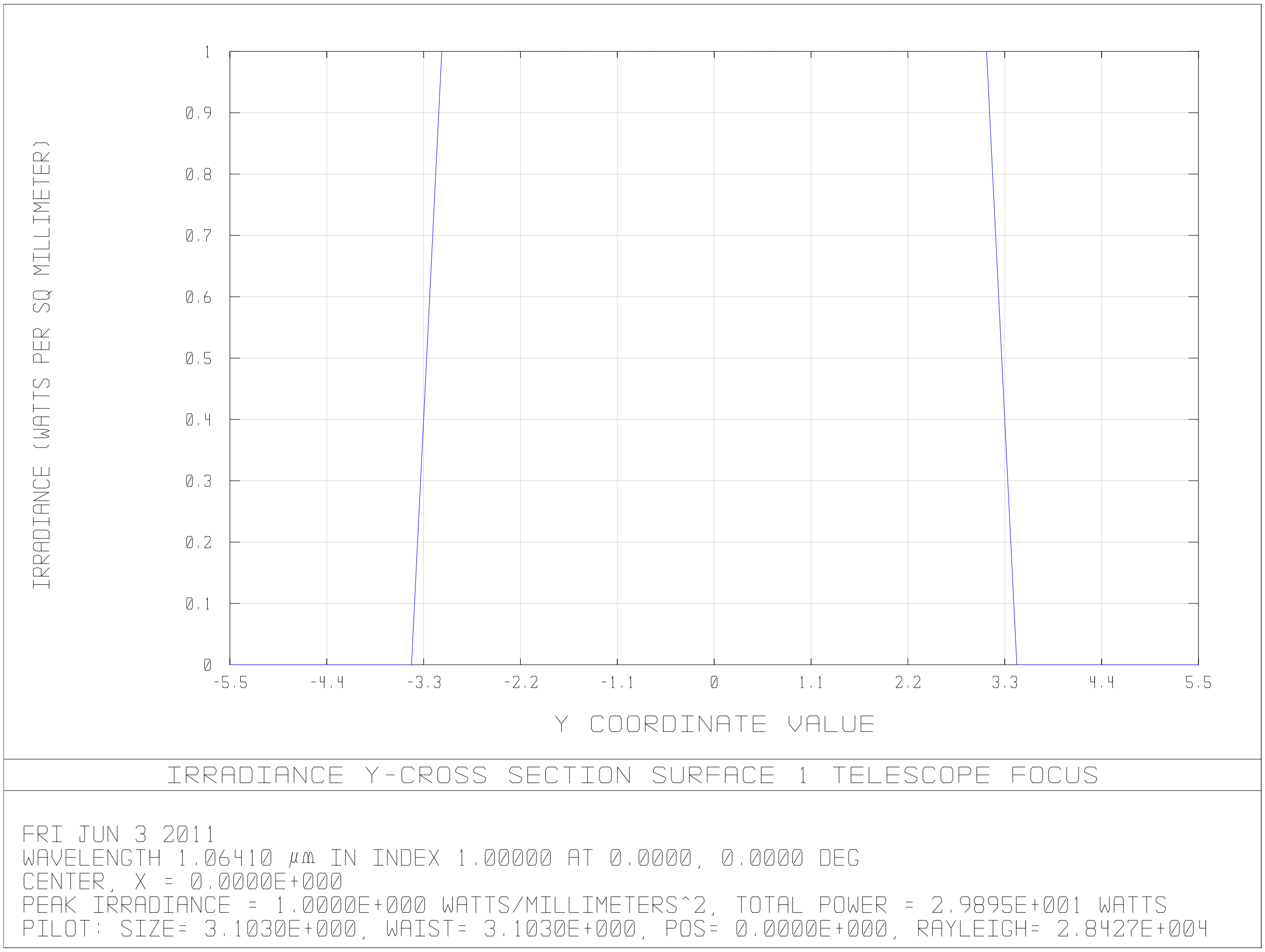

Figure 48: Top Hat Input beam: Profile

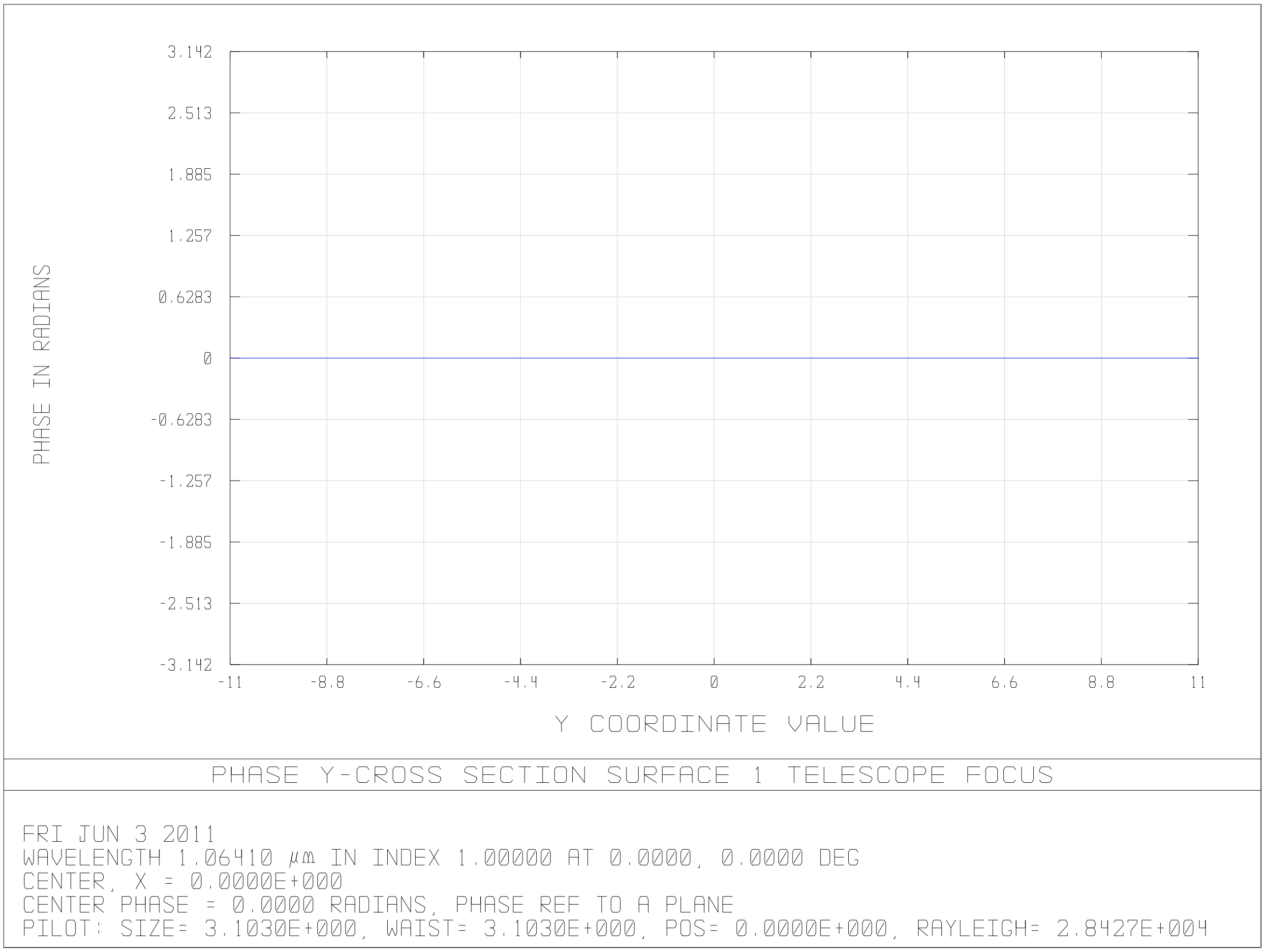

Figure 49: Top Hat Input beam: Phase

The output beam profile and phase after a double pass through the telescope are shown in Figure 50, Figure 51.

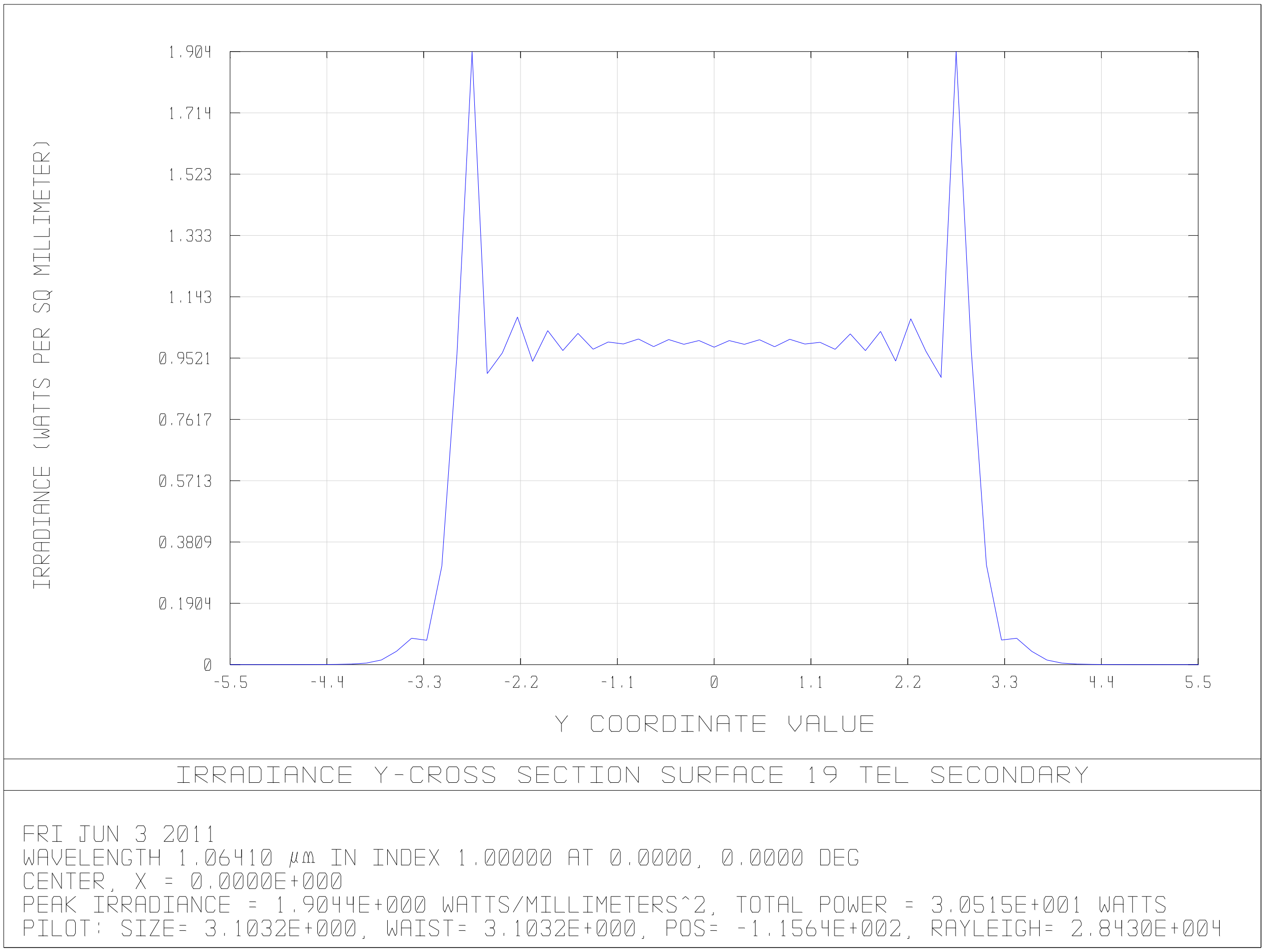

Figure 50: Top Hat Output beam: Profile

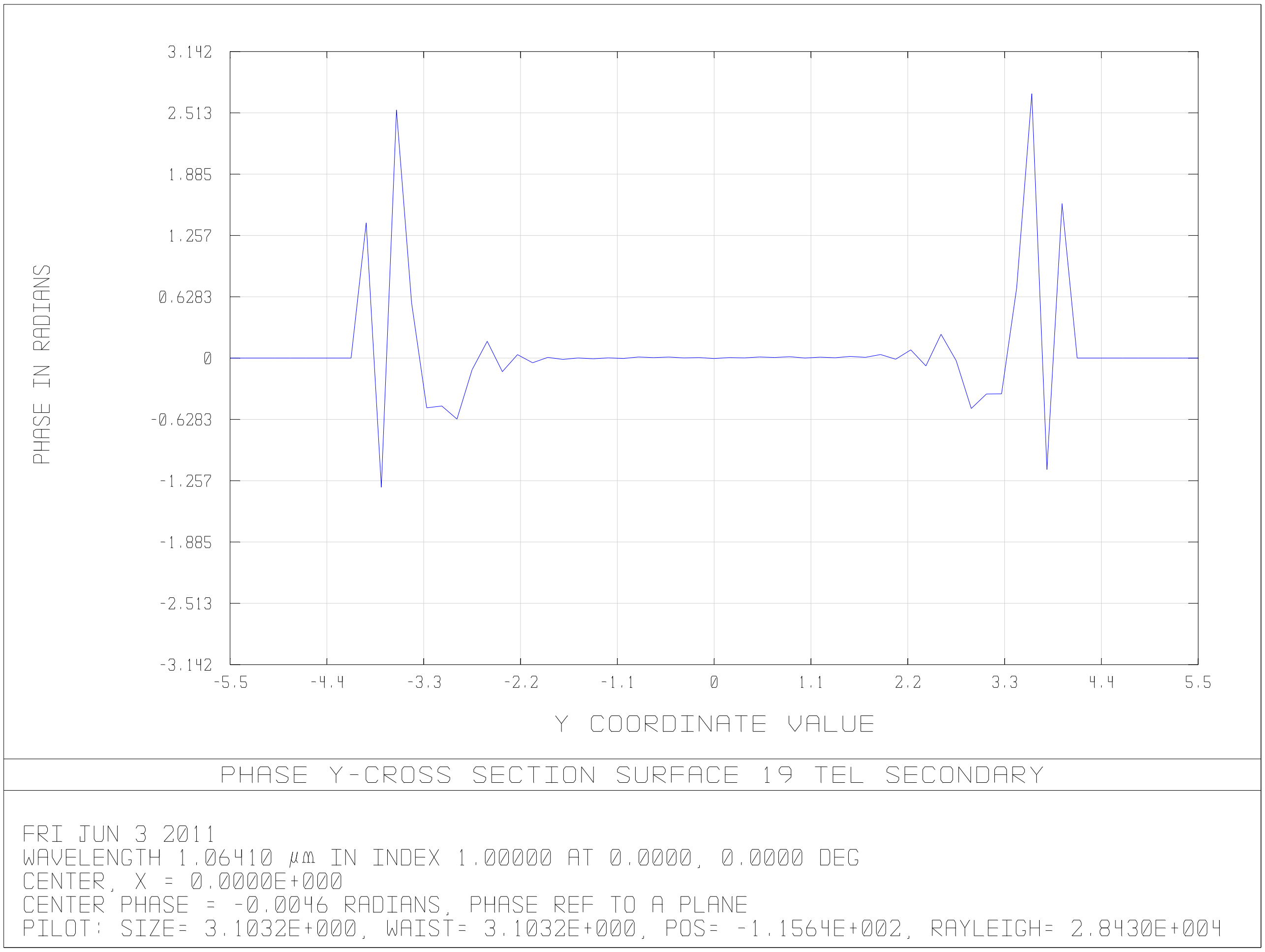

Figure 51: Top Hat Output beam: Phase

These results show that within the 60% central portion of the beam the output wavefront is flat, independent of the shape of the input beam profile. The non-Gaussian edges of the input beam cause diffraction effects on the edges of the output beam, as expected.

3.3.5 ABCD Matrix Gaussian Beam Propagation

3.3.5.1 Gaussian Beam Propagation from IFO Beam Waist to 2ndary Mirror of TMS Telescope

The ABCD matrix calculation was used to determine the parameters of an ideal TMS telescope.

A 1064 nm, 12.014 mm Gaussian beam waist was propagated 2161 m to the ETM HR surface; the beam radius at the ETM HR is 62.094 mm, and the radius of curvature of the beam is 2245 m concave toward the beam waist.

The telescope mirror spacing was set at 1902.585 to achieve a beam waist at the 2ndary mirror of the telescope; this focal distance agrees with the ZEMAX value. The Rayleigh range for the 3.103mm beam waist is 28 m.

wavelength, mm $\lambda := 1.06410^{-3}$

index of refraction of fused silica $n := 1.4496$

cavity length, mm $L := 399600$

radius of TMS M1, mm $R_{10} := -400($

radius of TMS M2, mm $R_{20} := 20($

radius1 of ETM, mm
ref: T0900043 $R1_{ETM} := -224500$

thickness of ETM mm $t_{ETM} := 20($

IFO beam waist size, mm $w_{IFO} = 12.014$

ABCD matrix from IFO beam waist to 2ndary mirror $M_{ifotms2} = \begin{pmatrix} 0.049 & 1.081\times 10^{5} \\ -8.919\times 10^{-6} & 0.736 \end{pmatrix}$

telescope defocus, mm $\Delta_f = 2.585$

TMS beam waist radius, mm $w_{ifotms0}(R_{10}, \Delta_f) = 3.103$

Raleigh range, mm $z_{Rtms0} = 2.844\times 10^{4}$

3.3.5.2 Astigmatic Focus of TMS Telescope with Spherical Mirrors

The incidence angles of the off axis reflecting TMS telescope will cause astigmatic foci at the focal plane of the Guoy lens because the tangential and saggital rays focus at different axial positions, and a large Guoy phase error. See Fundamentals of Optics, Jenkins & White.

off-axis angle, deg $\theta := 7.5($

Guoy Focus Lens, focal length $f_{focus} := 10($

tangential focus of TMS M1, mm $f_{10tan} := f_{10} \cdot \cos\left(\theta \cdot \frac{\pi}{180}\right)$

$f_{10tan} = -1.983\times 10^{3}$

saggital focus of TMS M1, mm

$$f_{10sag} := \frac{f_{10}}{\cos\left(\theta \cdot \frac{\pi}{180}\right)}$$

$$f_{10sag} = -2.017 \times 10^{3}$$

Astigmatic foci separation, mm

$$\Delta l_{focus}(R_{10}, \Delta_f) := l_{focusw0sag}(R_{10}, \Delta_f) - l_{focusw0tan}(R_{10}, \Delta_f)$$

$$\Delta l_{focus}(R_{10}, \Delta_f) = -2.819$$

Beam waist at Guoy lens, mm

$$w_{ifofocus0}(R_{10}, \Delta_f) = 0.017$$

Raleigh range, mm

$$z_{Rfocus0} := \pi \cdot \frac{w_{ifofocus0}(R_{10}, \Delta_f)^2}{\lambda}$$

$$z_{Rfocus0} = 0.843$$

Guoy Phase error

$$\Delta\phi_g := \operatorname{atan}\left(\frac{\Delta l_{focus}(R_{10}, \Delta_f)}{z_{Rfocus0}}\right) \cdot \frac{180}{\pi}$$

$$\Delta\phi_g = -73.355$$

4 Optical Aberration Theory

Astigmatic aberrations in the Transmon sensing beam will cause an apparent Guoy phase error in the Transmon detection system because the astigmatic beam has two focal planes shifted along the beam propagation direction.

There are several conventions for describing the Zernike polynomials, which differ in the normalizing constant for each term, and also in the order in which the polynomials are named.

4.1 ZEMAX Zernike Coefficients

ZEMAX defines two forms of the Zernike polynomials: Standard and Fringe Phase, which only differ in their normalyzing constant.

Zernike Standard Field Curvature Coefficient, Z4

$$Z_4 := \sqrt{3} \cdot \left(2 \cdot \rho^2 - 1\right)$$

Zernike Standard Astigmatism Coefficient, Z5 $Z_5 := \sqrt{6}\cdot\rho^2\cdot\sin(2\cdot\phi)$

Zernike Standard Astigmatism Coefficient, Z6 $Z_6 := \sqrt{6}\cdot\rho^2\cdot\cos(2\cdot\phi)$

Zernike Fringe Phase Field Curvature Coefficient, Z4 $Z_4 := 2\cdot\rho^2 - 1$

Zernike Fringe Phase Astigmatism Coefficient, Z5 $Z_5 := \rho^2\cdot\sin(2\cdot\phi)$

Zernike Fringe Phase Astigmatism Coefficient, Z6 $Z_6 := \rho^2\cdot\cos(2\cdot\phi)$

4.2 Shack-Hartmann Zernike Coefficients

The Shack-Hartmann software from Thorlabs uses a different definition of the Zernike polynomials, as stated in the software manual and derived from D. Malacara[1].

Zernike Malacara Defocus Coefficient, Z5 $Z_5 := \sqrt{3}\cdot\left(2\cdot\rho^2 - 1\right)$

Zernike Malacara Astigmatism Coefficient, Z4 $Z_4 := \sqrt{6}\cdot\rho^2\cdot\sin(2\cdot\phi)$

Zernike Malacara Astigmatism Coefficient, Z6 $Z_6 := \sqrt{6}\cdot\rho^2\cdot\cos(2\cdot\phi)$

4.3 Guoy Phase vs Astigmatic Focus Shift

According to Born and Wolf[2], the astigmatic focal shift on either side of the nominal focal position is proportional to the Zernike astigmatism coefficient and to the f-number of the focusing optical system.

astigmatic focal plane shift, m

[1] D. Malacara, *Optical Shop Testing*, 2nd ed., (John Wiley & Sons, Inc., New York, 1992

[2] M. Born & E. Wolf, *Principles of Optics*, 6th ed, p.472, (Pergamon Press, Oxford, New York, 1980)

$$\Delta f := \frac{R^2}{a^2} \cdot A_{p022} \cdot \lambda$$

where, R is the focal length of the focus lens, a is the semi-aperture diameter, and λ is the wavelength of light.

The Born and Wolf aberration coefficient is related to the standard Zernike Coefficient as follows:

Born and Wolfe Zernike Astigmatism coeff A22, waves $A_{p022} := 2 \cdot Z_5$

Therefore, the focal plane separation is proportional to the Z5 (and Z6) coefficients;

$$\Delta f := 4 \cdot \frac{R^2}{a^2} \cdot Z_5 \cdot \lambda$$

The Guoy phase difference between the two astigmatic foci is given by:

Guoy phase, deg $\varphi_G := \operatorname{atan}\left(\frac{\Delta f}{Z_R}\right) \cdot \frac{180}{\pi}$

where, the Rayleigh range is calculated by:

diffraction spot size, m $w_0 := \frac{\pi}{4} \cdot \lambda \cdot \frac{R}{2 \cdot a}$

Rayleigh range, m $Z_R := \frac{\pi \cdot {w_0}^2}{\lambda}$

In terms of the standard Born and Wolf Zernike coefficient, the Guoy phase shift is

Guoy phase, deg

$$\varphi_G := \operatorname{atan}\left(\frac{256 \cdot Z_5}{\pi^3}\right) \cdot \frac{180}{\pi}$$

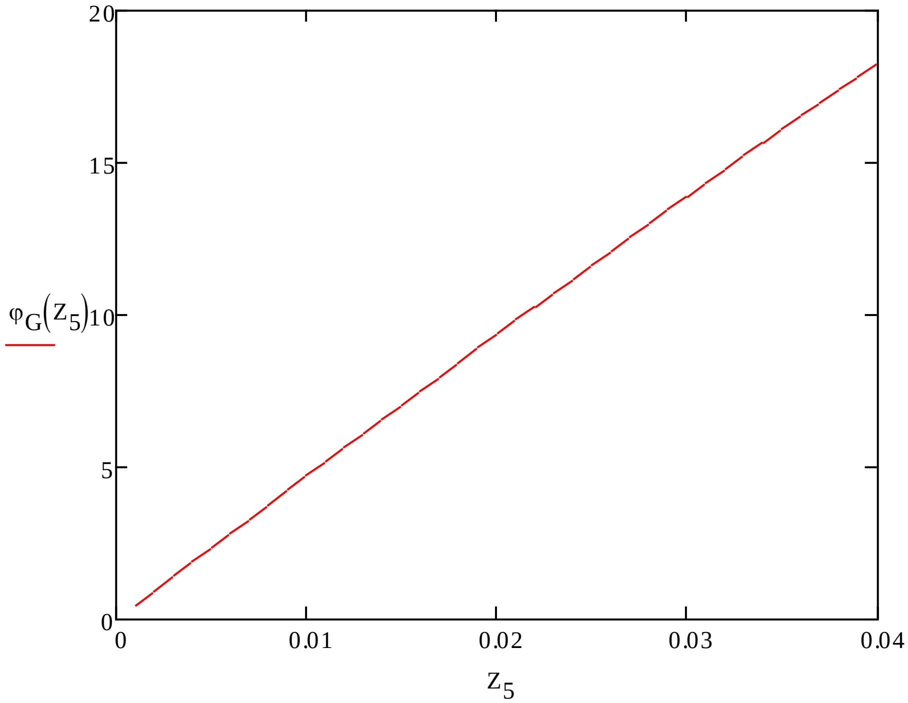

Figure 52: Guoy Phase vs Standard Zernike Astigmatism Coefficient